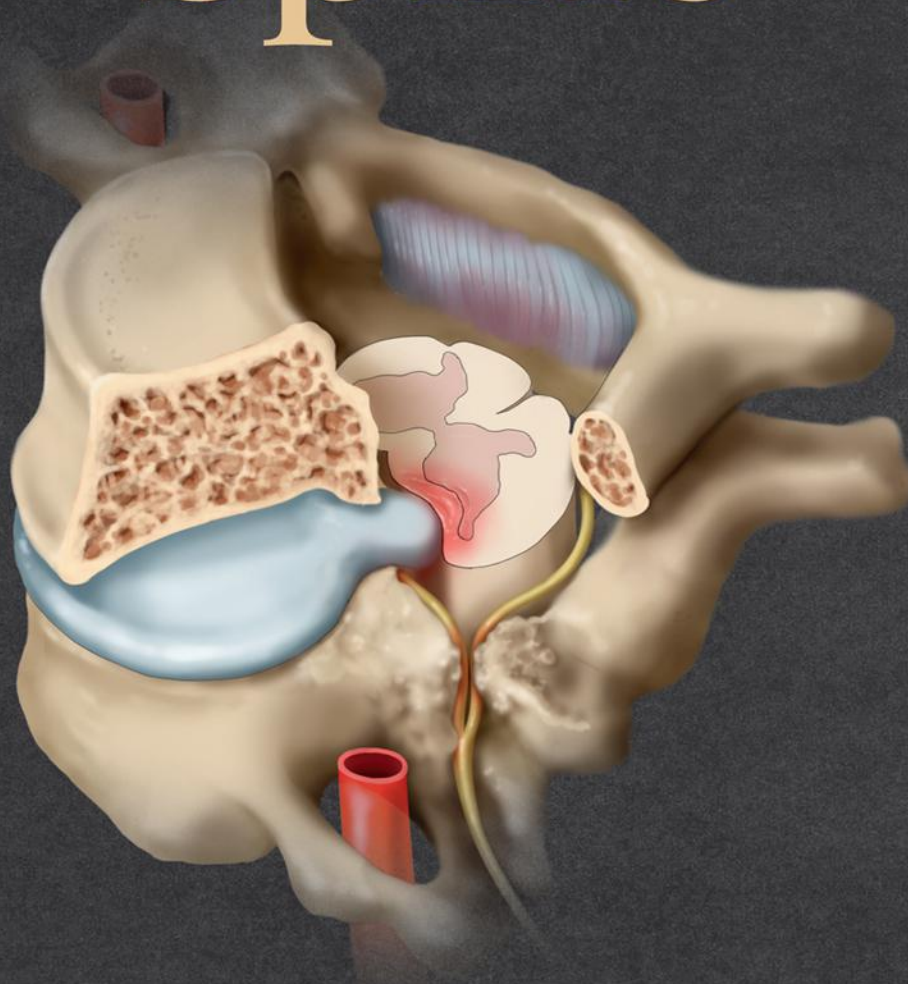


Get Full Access and More at

ExpertConsult.com

*Diagnostic Imaging*

# Spine

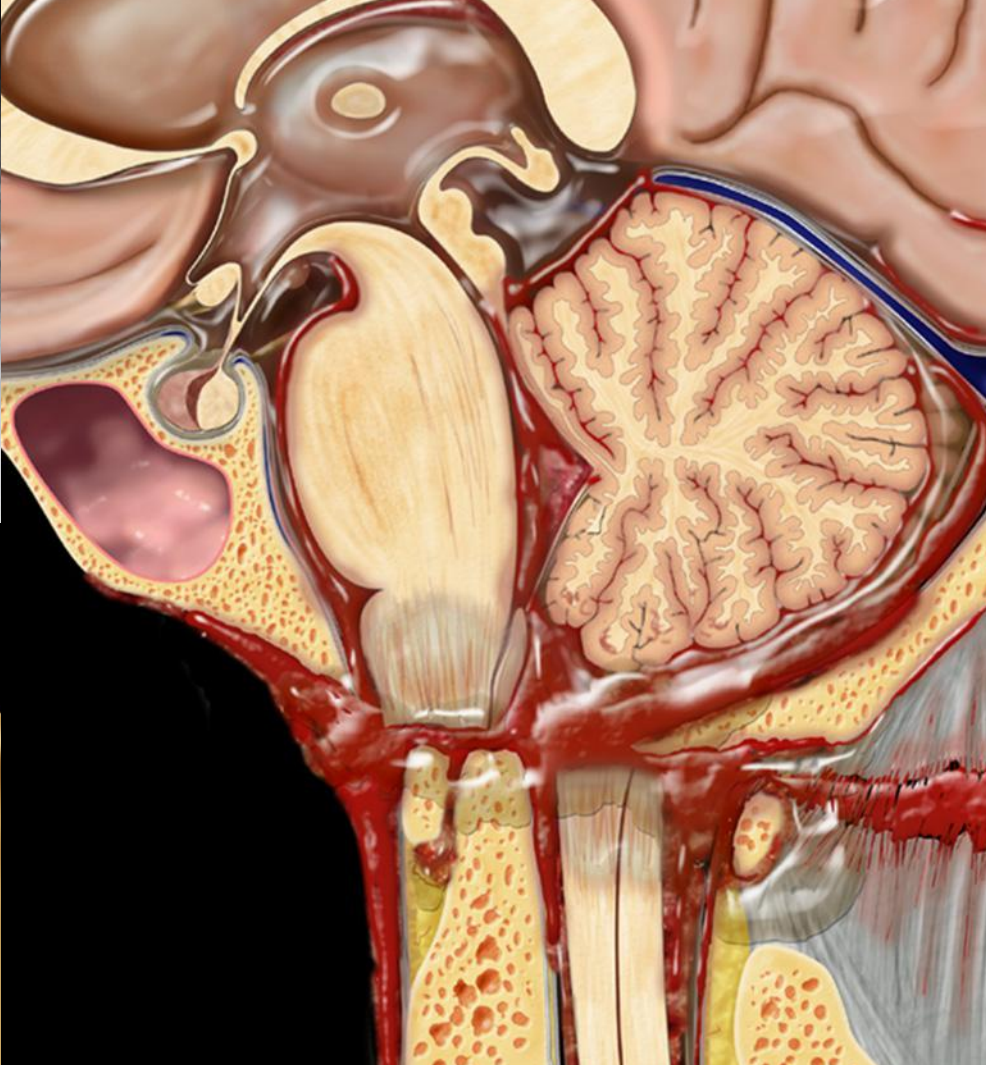
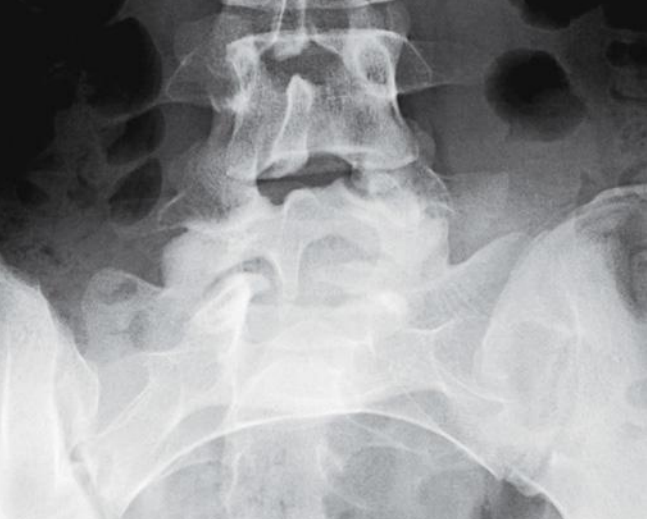


AMIRSYS®

ELSEVIER

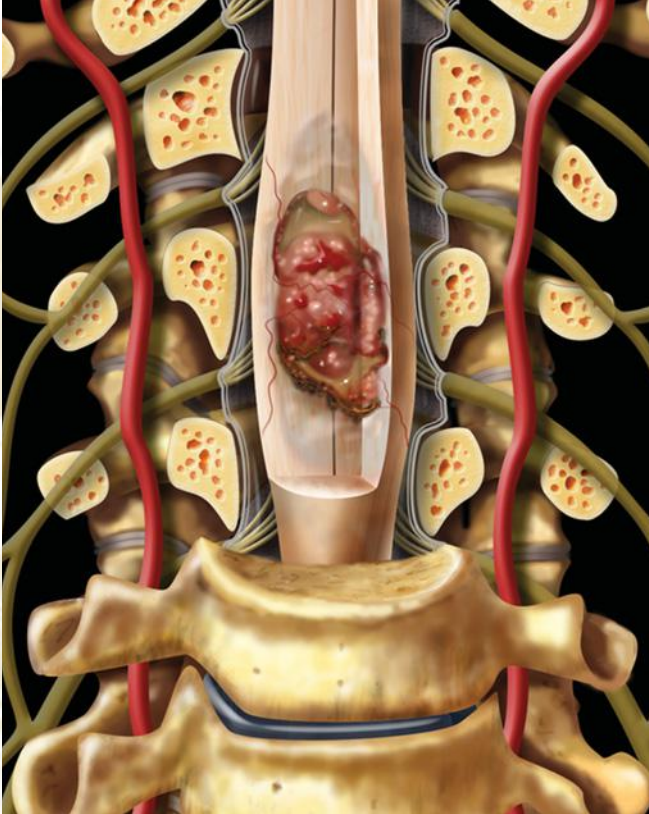
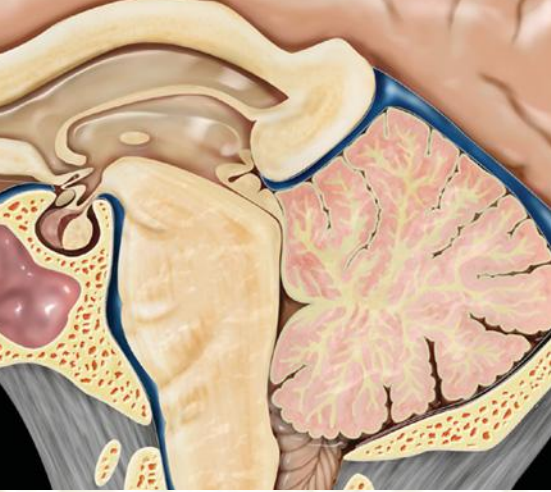
Ross | Moore





*Diagnostic Imaging*

# Spine



*Diagnostic Imaging*

# Spine

**Jeffrey S. Ross, MD**

Neuroradiology  
Barrow Neurological Institute  
St. Joseph's Hospital  
Phoenix, Arizona

**Kevin R. Moore, MD**

Pediatric Neuroradiology  
Intermountain Pediatric Imaging  
Primary Children's Hospital  
Salt Lake City, Utah



# ELSEVIER

1600 John F. Kennedy Blvd.  
Ste 1800  
Philadelphia, PA 19103-2899

DIAGNOSTIC IMAGING: SPINE, THIRD EDITION

ISBN: 978-0-323-37705-8

Copyright © 2015 by Elsevier. All rights reserved.

No part of this publication may be reproduced or transmitted in any form or by any means, electronic or mechanical, including photocopying, recording, or any information storage and retrieval system, without permission in writing from the publisher. Details on how to seek permission, further information about the Publisher's permissions policies and our arrangements with organizations such as the Copyright Clearance Center and the Copyright Licensing Agency, can be found at our website: [www.elsevier.com/permissions](http://www.elsevier.com/permissions).

This book and the individual contributions contained in it are protected under copyright by the Publisher (other than as may be noted herein).

## Notices

Knowledge and best practice in this field are constantly changing. As new research and experience broaden our understanding, changes in research methods, professional practices, or medical treatment may become necessary.

Practitioners and researchers must always rely on their own experience and knowledge in evaluating and using any information, methods, compounds, or experiments described herein. In using such information or methods they should be mindful of their own safety and the safety of others, including parties for whom they have a professional responsibility.

With respect to any drug or pharmaceutical products identified, readers are advised to check the most current information provided (i) on procedures featured or (ii) by the manufacturer of each product to be administered, to verify the recommended dose or formula, the method and duration of administration, and contraindications. It is the responsibility of practitioners, relying on their own experience and knowledge of their patients, to make diagnoses, to determine dosages and the best treatment for each individual patient, and to take all appropriate safety precautions.

To the fullest extent of the law, neither the Publisher nor the authors, contributors, or editors, assume any liability for any injury and/or damage to persons or property as a matter of products liability, negligence or otherwise, or from any use or operation of any methods, products, instructions, or ideas contained in the material herein.

## Publisher Cataloging-in-Publication Data

Diagnostic imaging. Spine / [edited by] Jeffrey S. Ross and Kevin R. Moore.

3rd edition.

pages ; cm

Spine

Includes bibliographical references and index.

ISBN 978-0-323-37705-8 (hardback)

1. Spine--Imaging--Handbooks, manuals, etc. 2. Diagnostic imaging.

I. Ross, Jeffrey S. (Jeffrey Stuart). II. Moore, Kevin R. III. Title: Spine.

[DNLM: 1. Spinal Diseases--diagnosis--Handbooks. 2. Magnetic Resonance Imaging--Handbooks.

3. Spine--anatomy & histology--Handbooks. WE 725]

RD768.D535 2015

616.7/30754--dc23

International Standard Book Number: 978-0-323-37705-8

Cover Designer: Tom M. Olson, BA

Cover Art: Laura C. Sesto, MA

Printed in Canada by Friesens, Altona, Manitoba, Canada

Last digit is the print number: 9 8 7 6 5 4 3 2 1



# Dedications

*"Let the wise hear and increase in learning, and the one  
who understands obtain guidance."*

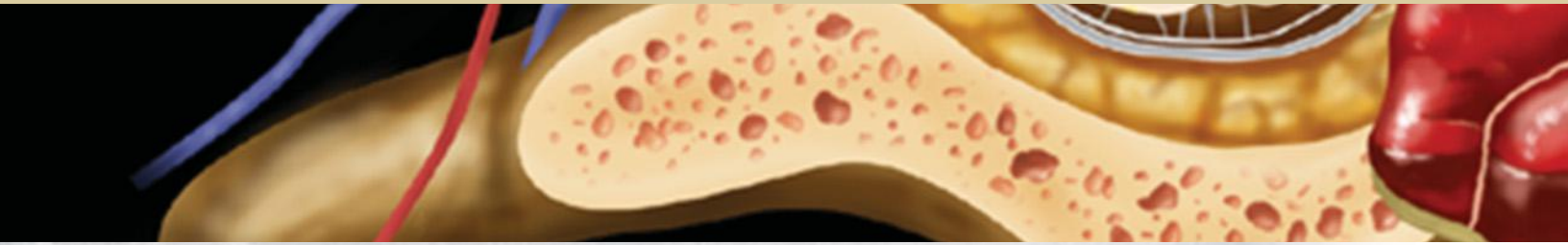
*Proverbs 1:5*

**JSR**

*A project of this magnitude reflects the hard efforts  
of many underrecognized people. I extend my deepest  
gratitude to all of you – thank you!*

**KRM**





# Contributing Authors



## **Lubdha M. Shah, MD**

Associate Professor of Radiology  
Division of Neuroradiology  
University of Utah School of Medicine  
Salt Lake City, Utah

## **Bryson Borg, MD**

Fairfield, California

## **Julia Crim, MD**

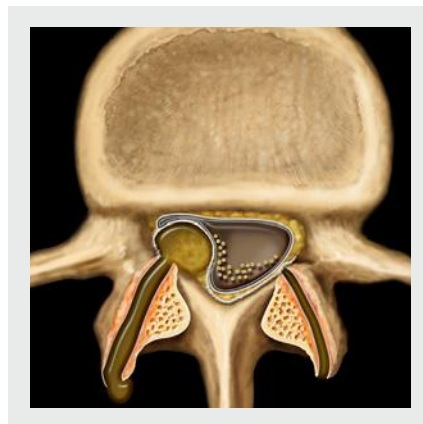
Chief of Musculoskeletal Radiology  
Professor of Radiology  
University of Missouri at Columbia  
Columbia, Missouri

## **Cheryl Petersilge, MD, MBA**

Clinical Professor of Radiology  
Cleveland Clinic Lerner College of Medicine  
Case Western Reserve University  
Cleveland, Ohio

## **A. Carl Merrow, MD**

Corning Benton Chair for Radiology Education  
Cincinnati Children's Hospital Medical Center  
Associate Professor of Clinical Radiology  
University of Cincinnati College of Medicine  
Cincinnati, Ohio







# Preface



Welcome to the third edition of *Diagnostic Imaging: Spine*. Five years have passed since the second edition, and eleven years have flown by since the first edition was published. This edition is a refresh with new images, new diagnoses, and updated text and references. The same excellent Amirsys formatting is present, with individual diagnoses capable of standing alone but with a logical integration within the larger sections. The Key Facts box retains its visual prominence at the beginning of each diagnosis, allowing for a quick scan of the most important bullet points when time is short (and when is it not?). The text format remains in the hallmark Amirsys bulleted form that allows a large amount of important information to be displayed in an easy-to-use and inviting layout. Prose text chapters are included for the introduction to major sections, which are color coded, and the use of tables allows quick scanning for important data and measurements.

Our coauthors and the staff at Amirsys/Elsevier have been amazing to work with, and we have been very fortunate to be able to interact with and learn from such a fantastic team. We hope you find this edition useful not only as a reference, but also as an integral assistant in your daily practice.

## **Jeffrey S. Ross, MD**

Neuroradiology  
Barrow Neurological Institute  
St. Joseph's Hospital  
Phoenix, Arizona

## **Kevin R. Moore, MD**

Pediatric Neuroradiology  
Intermountain Pediatric Imaging  
Primary Children's Hospital  
Salt Lake City, Utah





# Acknowledgements

## **Text Editing**

Dave L. Chance, MA, ELS  
Arthur G. Gelsing, MA  
Nina I. Bennett, BA  
Sarah J. Connor, BA  
Tricia L. Cannon, BA  
Terry W. Ferrell, MS  
Lisa A. Gervais, BS

## **Image Editing**

Jeffrey J. Marmorstone, BS  
Lisa A. M. Steadman, BS

## **Medical Editors**

Michal Klysik, MD  
Karthik C. Kumar, MD

## **Illustrations**

Richard Coombs, MS  
Lane R. Bennion, MS  
Laura C. Sesto, MA

## **Art Direction and Design**

Tom M. Olson, BA  
Laura C. Sesto, MA

## **Lead Editor**

Nina I. Bennett, BA

## **Production Coordinators**

Angela G. Terry, BA  
Rebecca L. Hutchinson, BA

ELSEVIER





# Sections

## **PART I: Congenital and Genetic Disorders**

SECTION 1: Congenital

SECTION 2: Scoliosis and Kyphosis

## **PART II: Trauma**

SECTION 1: Vertebral Column, Discs, and Paraspinal Muscle

SECTION 2: Cord, Dura, and Vessels

## **PART III: Degenerative Diseases and Arthritides**

SECTION 1: Degenerative Diseases

SECTION 2: Spondylolisthesis and Spondylolysis

SECTION 3: Inflammatory, Crystalline, and Miscellaneous Arthritides

## **PART IV: Infection and Inflammatory Disorders**

SECTION 1: Infections

SECTION 2: Inflammatory and Autoimmune Disorders

## **PART V: Neoplasms, Cysts, and Other Masses**

SECTION 1: Neoplasms

SECTION 2: Nonneoplastic Cysts and Tumor Mimics

SECTION 3: Vascular and Systemic Disorders

## **PART VI: Peripheral Nerve and Plexus**

SECTION 1: Plexus and Peripheral Nerve Lesions

## **PART VII: Spine Postprocedural Imaging**

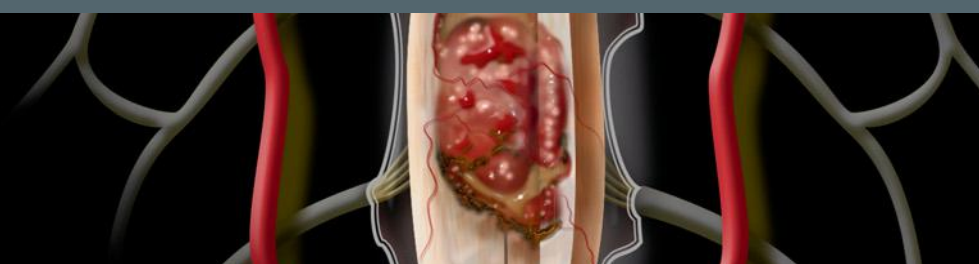
SECTION 1: Postoperative Imaging and Complications

SECTION 2: Hardware

SECTION 3: Post Radiation and Chemotherapy Complications



# TABLE OF CONTENTS



## Part I: Congenital and Genetic Disorders

### SECTION 1: CONGENITAL

#### NORMAL ANATOMICAL VARIATIONS

- 4 **Normal Anatomy**  
*Jeffrey S. Ross, MD*
- 10 **Measurement Techniques**  
*Jeffrey S. Ross, MD*
- 16 **MR Artifacts**  
*Kevin R. Moore, MD*
- 22 **Normal Variant**  
*Kevin R. Moore, MD*
- 26 **Craniovertebral Junction Variants**  
*Kevin R. Moore, MD*
- 30 **Ponticulus Posticus**  
*Kevin R. Moore, MD*
- 32 **Ossiculum Terminale**  
*Kevin R. Moore, MD*
- 34 **Conjoined Nerve Roots**  
*Kevin R. Moore, MD*
- 38 **Limbus Vertebra**  
*Kevin R. Moore, MD*
- 42 **Filum Terminale Fibrolipoma**  
*Kevin R. Moore, MD*
- 44 **Bone Island**  
*Kevin R. Moore, MD*
- 46 **Ventriculus Terminalis**  
*Kevin R. Moore, MD*

#### CHIARI DISORDERS

- 50 **Chiari 0**  
*Kevin R. Moore, MD*
- 52 **Chiari 1**  
*Kevin R. Moore, MD*
- 56 **Complex Chiari**  
*Kevin R. Moore, MD*
- 58 **Chiari 2**  
*Kevin R. Moore, MD*
- 62 **Chiari 3**  
*Kevin R. Moore, MD*

#### ABNORMALITIES OF NEURULATION

- 64 **Approach to Spine and Spinal Cord Development**  
*Kevin R. Moore, MD*
- 72 **Myelomeningocele**  
*Kevin R. Moore, MD*

- 76 **Lipomyelomeningocele**  
*Kevin R. Moore, MD*
- 80 **Lipoma**  
*Kevin R. Moore, MD*
- 84 **Dorsal Dermal Sinus**  
*Kevin R. Moore, MD*
- 88 **Simple Coccygeal Dimple**  
*Kevin R. Moore, MD*
- 92 **Dermoid Cysts**  
*Kevin R. Moore, MD*
- 96 **Epidermoid Cysts**  
*Kevin R. Moore, MD*

#### ANOMALIES OF THE CAUDAL CELL MESS

- 100 **Tethered Spinal Cord**  
*Kevin R. Moore, MD*
- 104 **Segmental Spinal Dysgenesis**  
*Kevin R. Moore, MD*
- 108 **Caudal Regression Syndrome**  
*Kevin R. Moore, MD*
- 112 **Terminal Myelocystocele**  
*Kevin R. Moore, MD*
- 116 **Anterior Sacral Meningocele**  
*Kevin R. Moore, MD*
- 120 **Sacral Extradural Arachnoid Cyst**  
*Kevin R. Moore, MD*
- 124 **Sacrococcygeal Teratoma**  
*Kevin R. Moore, MD*

#### ANOMALIES OF NOTOCHORD AND VERTEBRAL FORMATION

- 128 **Craniovertebral Junction Embryology**  
*Kevin R. Moore, MD*
- 132 **Paracondylar Process**  
*Jeffrey S. Ross, MD*
- 134 **Split Atlas**  
*Kevin R. Moore, MD*
- 136 **Klippel-Feil Spectrum**  
*Kevin R. Moore, MD*
- 140 **Failure of Vertebral Formation**  
*Kevin R. Moore, MD*
- 144 **Vertebral Segmentation Failure**  
*Kevin R. Moore, MD*
- 148 **Diastematomyelia**  
*Kevin R. Moore, MD*
- 152 **Partial Vertebral Duplication**  
*Kevin R. Moore, MD*
- 154 **Incomplete Fusion, Posterior Element**  
*Kevin R. Moore, MD*

# TABLE OF CONTENTS

- 156 **Neurenteric Cyst**  
*Kevin R. Moore, MD*

## DEVELOPMENTAL ABNORMALITIES

- 160 **Os Odontoideum**  
*Kevin R. Moore, MD*
- 164 **Lateral Meningocele**  
*Kevin R. Moore, MD*
- 168 **Dorsal Spinal Meningocele**  
*Kevin R. Moore, MD*
- 172 **Dural Dysplasia**  
*Kevin R. Moore, MD*

## GENETIC DISORDERS

- 176 **Neurofibromatosis Type 1**  
*Kevin R. Moore, MD*
- 180 **Neurofibromatosis Type 2**  
*Jeffrey S. Ross, MD*
- 186 **Achondroplasia**  
*Bryson Borg, MD*
- 190 **Mucopolysaccharidoses**  
*Bryson Borg, MD*
- 194 **Sickle Cell Disease**  
*Bryson Borg, MD*
- 198 **Osteogenesis Imperfecta**  
*Carl Mellow, MD*
- 202 **Tuberous Sclerosis**  
*Jeffrey S. Ross, MD*
- 206 **Osteopetrosis**  
*Kevin R. Moore, MD*
- 208 **Gaucher Disease**  
*Kevin R. Moore, MD*
- 210 **Ochronosis**  
*Kevin R. Moore, MD*
- 212 **Connective Tissue Disorders**  
*Kevin R. Moore, MD*
- 216 **Spondyloepiphyseal Dysplasia**  
*Kevin R. Moore, MD*
- 220 **Thanatophoric Dwarfism**  
*Kevin R. Moore, MD*

## SECTION 2: SCOLIOSIS AND KYPHOSIS

- 224 **Introduction to Scoliosis**  
*Julia Crim, MD*
- 228 **Scoliosis**  
*Kevin R. Moore, MD*
- 232 **Kyphosis**  
*Kevin R. Moore, MD*
- 234 **Degenerative Scoliosis**  
*Jeffrey S. Ross, MD*
- 238 **Flat Back Syndrome**  
*Lubdha M. Shah, MD*
- 240 **Scoliosis Instrumentation**  
*Lubdha M. Shah, MD*

## Part II: Trauma

### SECTION 1: VERTEBRAL COLUMN, DISCS, AND PARASPINAL MUSCLE

- 246 **Fracture Classification**  
*Jeffrey S. Ross, MD*
- 252 **Atlantooccipital Dislocation**  
*Julia Crim, MD*
- 256 **Ligamentous Injury**  
*Bryson Borg, MD and Jeffrey S. Ross, MD*
- 260 **Occipital Condyle Fracture**  
*Bryson Borg, MD and Jeffrey S. Ross, MD*
- 264 **Jefferson C1 Fracture**  
*Bryson Borg, MD*
- 268 **Atlantoaxial Rotatory Fixation**  
*Jeffrey S. Ross, MD*
- 274 **Odontoid C2 Fracture**  
*Bryson Borg, MD and Jeffrey S. Ross, MD*
- 278 **Burst C2 Fracture**  
*Bryson Borg, MD*
- 282 **Hangman's C2 Fracture**  
*Bryson Borg, MD*
- 286 **Apophyseal Ring Fracture**  
*Kevin R. Moore, MD*
- 290 **Cervical Hyperflexion Injury**  
*Jeffrey S. Ross, MD*
- 296 **Cervical Hyperextension Injury**  
*Jeffrey S. Ross, MD*
- 300 **Cervical Hyperextension-Rotation Injury**  
*Bryson Borg, MD*
- 302 **Cervical Burst Fracture**  
*Jeffrey S. Ross, MD*
- 306 **Cervical Hyperflexion-Rotation Injury**  
*Bryson Borg, MD*
- 308 **Cervical Lateral Flexion Injury**  
*Jeffrey S. Ross, MD*
- 310 **Cervical Posterior Column Injury**  
*Bryson Borg, MD and Jeffrey S. Ross, MD*
- 312 **Traumatic Disc Herniation**  
*Bryson Borg, MD*
- 314 **Thoracic and Lumbar Burst Fracture**  
*Julia Crim, MD and Jeffrey S. Ross, MD*
- 318 **Facet-Lamina Thoracolumbar Fracture**  
*Bryson Borg, MD*
- 320 **Fracture Dislocation**  
*Bryson Borg, MD*
- 322 **Chance Fracture**  
*Julia Crim, MD and Jeffrey S. Ross, MD*
- 328 **Thoracic and Lumbar Hyperextension Injury**  
*Bryson Borg, MD and Jeffrey S. Ross, MD*
- 330 **Anterior Compression Fracture**  
*Julia Crim, MD*
- 334 **Lateral Compression Fracture**  
*Julia Crim, MD and Jeffrey S. Ross, MD*
- 336 **Lumbar Facet-Posterior Fracture**  
*Bryson Borg, MD and Jeffrey S. Ross, MD*
- 338 **Sacral Traumatic Fracture**  
*Julia Crim, MD*

# TABLE OF CONTENTS

- 342 **Pedicle Stress Fracture**  
*Bryson Borg, MD and Jeffrey S. Ross, MD*
- 346 **Sacral Insufficiency Fracture**  
*Bryson Borg, MD*

## SECTION 2: CORD, DURA, AND VESSELS

- 352 **SCIWORA**  
*Kevin R. Moore, MD*
- 356 **Post-Traumatic Syrinx**  
*Jeffrey S. Ross, MD*
- 360 **Presyrinx Edema**  
*Jeffrey S. Ross, MD*
- 364 **Spinal Cord Contusion-Hematoma**  
*Bryson Borg, MD and Jeffrey S. Ross, MD*
- 370 **Idiopathic Spinal Cord Herniation**  
*Jeffrey S. Ross, MD*
- 374 **Central Spinal Cord Syndrome**  
*Bryson Borg, MD and Jeffrey S. Ross, MD*
- 378 **Traumatic Dural Tear**  
*Bryson Borg, MD and Jeffrey S. Ross, MD*
- 382 **Traumatic Epidural Hematoma**  
*Kevin R. Moore, MD*
- 386 **Traumatic Subdural Hematoma**  
*Bryson Borg, MD*
- 388 **Vascular Injury, Cervical**  
*Bryson Borg, MD and Jeffrey S. Ross, MD*
- 394 **Traumatic Arteriovenous Fistula**  
*Bryson Borg, MD*
- 396 **Wallerian Degeneration**  
*Jeffrey S. Ross, MD*

## Part III: Degenerative Diseases and Arthritides

### SECTION 1: DEGENERATIVE DISEASES

- 400 **Nomenclature of Degenerative Disc Disease**  
*Jeffrey S. Ross, MD*
- 404 **Degenerative Disc Disease**  
*Jeffrey S. Ross, MD*
- 410 **Degenerative Endplate Changes**  
*Jeffrey S. Ross, MD*
- 414 **Degenerative Arthritis of the CVJ**  
*Cheryl A. Petersilge, MD, MBA*
- 418 **Disc Bulge**  
*Jeffrey S. Ross, MD*
- 422 **Anular Fissure, Intervertebral Disc**  
*Jeffrey S. Ross, MD*
- 426 **Cervical Intervertebral Disc Herniation**  
*Jeffrey S. Ross, MD*
- 432 **Thoracic Intervertebral Disc Herniation**  
*Jeffrey S. Ross, MD*
- 436 **Lumbar Intervertebral Disc Herniation**  
*Jeffrey S. Ross, MD*
- 442 **Intervertebral Disc Extrusion, Foraminal**  
*Jeffrey S. Ross, MD*
- 446 **Cervical Facet Arthropathy**  
*Jeffrey S. Ross, MD*

- 450 **Lumbar Facet Arthropathy**  
*Jeffrey S. Ross, MD*
- 454 **Facet Joint Synovial Cyst**  
*Jeffrey S. Ross, MD*
- 460 **Baastrup Disease**  
*Jeffrey S. Ross, MD*
- 464 **Bertolotti Syndrome**  
*Jeffrey S. Ross, MD*
- 466 **Schmorl Node**  
*Jeffrey S. Ross, MD and Kevin R. Moore, MD*
- 470 **Scheuermann Disease**  
*Jeffrey S. Ross, MD and Kevin R. Moore, MD*
- 474 **Acquired Lumbar Central Stenosis**  
*Jeffrey S. Ross, MD*
- 478 **Congenital Spinal Stenosis**  
*Jeffrey S. Ross, MD*
- 484 **Cervical Spondylosis**  
*Jeffrey S. Ross, MD*
- 490 **DISH**  
*Jeffrey S. Ross, MD*
- 494 **OPLL**  
*Jeffrey S. Ross, MD*
- 498 **Ossification Ligamentum Flavum**  
*Jeffrey S. Ross, MD*
- 502 **Periodontoid Pseudotumor**  
*Jeffrey S. Ross, MD*

### SECTION 2: SPONDYLOLISTHESIS AND SPONDYLOLYSIS

- 508 **Spondylolisthesis**  
*Jeffrey S. Ross, MD*
- 512 **Spondylolysis**  
*Jeffrey S. Ross, MD*
- 516 **Instability**  
*Jeffrey S. Ross, MD*

### SECTION 3: INFLAMMATORY, CRYSTALLINE, AND MISCELLANEOUS ARTHRITIDES

- 522 **Adult Rheumatoid Arthritis**  
*Jeffrey S. Ross, MD*
- 528 **Juvenile Idiopathic Arthritis**  
*Julia Crim, MD and Jeffrey S. Ross, MD*
- 534 **Spondyloarthropathy**  
*Jeffrey S. Ross, MD*
- 540 **Neurogenic (Charcot) Arthropathy**  
*Julia Crim, MD*
- 544 **Hemodialysis Spondyloarthropathy**  
*Julia Crim, MD and Jeffrey S. Ross, MD*
- 546 **Ankylosing Spondylitis**  
*Jeffrey S. Ross, MD*
- 550 **CPPD**  
*Jeffrey S. Ross, MD*
- 556 **Gout**  
*Julia Crim, MD*
- 558 **Longus Colli Calcific Tendinitis**  
*Julia Crim, MD and Jeffrey S. Ross, MD*



# TABLE OF CONTENTS

## Part IV: Infection and Inflammatory Disorders

### SECTION 1: INFECTIONS

- 564 **Pathways of Spread**  
*Jeffrey S. Ross, MD*
- 568 **Spinal Meningitis**  
*Lubdha M. Shah, MD*
- 572 **Pyogenic Osteomyelitis**  
*Lubdha M. Shah, MD and Jeffrey S. Ross, MD*
- 578 **Tuberculous Osteomyelitis**  
*Lubdha M. Shah, MD and Jeffrey S. Ross, MD*
- 584 **Fungal and Miscellaneous Osteomyelitis**  
*Kevin R. Moore, MD*
- 586 **Osteomyelitis, C1-C2**  
*Lubdha M. Shah, MD*
- 590 **Brucellar Spondylitis**  
*Lubdha M. Shah, MD and Kevin R. Moore, MD*
- 592 **Septic Facet Joint Arthritis**  
*Lubdha M. Shah, MD and Jeffrey S. Ross, MD*
- 598 **Paraspinal Abscess**  
*Lubdha M. Shah, MD*
- 602 **Epidural Abscess**  
*Lubdha M. Shah, MD*
- 608 **Subdural Abscess**  
*Lubdha M. Shah, MD and Kevin R. Moore, MD*
- 612 **Abscess, Spinal Cord**  
*Jeffrey S. Ross, MD*
- 616 **Viral Myelitis**  
*Lubdha M. Shah, MD and Kevin R. Moore, MD*
- 620 **HIV Myelitis**  
*Lubdha M. Shah, MD*
- 624 **Syphilitic Myelitis**  
*Jeffrey S. Ross, MD*
- 626 **Opportunistic Infections**  
*Lubdha M. Shah, MD and Kevin R. Moore, MD*
- 630 **Echinococcosis**  
*Lubdha M. Shah, MD*
- 634 **Schistosomiasis**  
*Lubdha M. Shah, MD*
- 638 **Cysticercosis**  
*Lubdha M. Shah, MD*

### SECTION 2: INFLAMMATORY AND AUTOIMMUNE DISORDERS

- 644 **Acute Transverse Myelopathy**  
*Jeffrey S. Ross, MD*
- 648 **Idiopathic Acute Transverse Myelitis**  
*Kevin R. Moore, MD*
- 652 **Multiple Sclerosis**  
*Lubdha M. Shah, MD and Kevin R. Moore, MD*
- 656 **Neuromyelitis Optica**  
*Lubdha M. Shah, MD and Jeffrey S. Ross, MD*
- 660 **ADEM**  
*Jeffrey S. Ross, MD*
- 664 **Guillain-Barré Syndrome**  
*Lubdha M. Shah, MD and Kevin R. Moore, MD*

- 668 **CIDP**  
*Jeffrey S. Ross, MD*
- 672 **Sarcoidosis**  
*Lubdha M. Shah, MD and Jeffrey S. Ross, MD*
- 678 **Subacute Combined Degeneration**  
*Lubdha M. Shah, MD*
- 682 **Chronic Recurrent Multifocal Osteomyelitis**  
*Jeffrey S. Ross, MD*
- 684 **Grisel Syndrome**  
*Cheryl A. Petersilge, MD, MBA*
- 686 **Paraneoplastic Myelopathy**  
*Jeffrey S. Ross, MD*

## Part V: Neoplasms, Cysts, and Other Masses

### SECTION 1: NEOPLASMS

#### INTRODUCTION AND OVERVIEW

- 690 **Spread of Neoplasms**  
*Jeffrey S. Ross, MD*

#### EXTRADURAL

- 694 **Blastic Osseous Metastases**  
*Bryson Borg, MD*
- 698 **Lytic Osseous Metastases**  
*Bryson Borg, MD*
- 702 **Hemangioma**  
*Bryson Borg, MD*
- 706 **Osteoid Osteoma**  
*Julia Crim, MD and Jeffrey S. Ross, MD*
- 712 **Osteblastoma**  
*Kevin R. Moore, MD*
- 716 **Aneurysmal Bone Cyst**  
*Jeffrey S. Ross, MD*
- 720 **Giant Cell Tumor**  
*Jeffrey S. Ross, MD*
- 724 **Osteochondroma**  
*Bryson Borg, MD and Kevin R. Moore, MD*
- 728 **Chondrosarcoma**  
*Bryson Borg, MD and Kevin R. Moore, MD*
- 732 **Osteosarcoma**  
*Julia Crim, MD and Kevin R. Moore, MD*
- 736 **Chordoma**  
*Bryson Borg, MD and Kevin R. Moore, MD*
- 742 **Ewing Sarcoma**  
*Julia Crim, MD*
- 746 **Lymphoma**  
*Lubdha M. Shah, MD and Jeffrey S. Ross, MD*
- 752 **Leukemia**  
*Lubdha M. Shah, MD*
- 756 **Plasmacytoma**  
*Lubdha M. Shah, MD and Kevin R. Moore, MD*
- 760 **Multiple Myeloma**  
*Lubdha M. Shah, MD*
- 764 **Neuroblastic Tumor**  
*Lubdha M. Shah, MD and Kevin R. Moore, MD*

# TABLE OF CONTENTS

**768 Langerhans Cell Histiocytosis**  
*Lubdha M. Shah, MD and Kevin R. Moore, MD*

**772 Angiolipoma**  
*Lubdha M. Shah, MD and Kevin R. Moore, MD*

## INTRADURAL EXTRAMEDULLARY

**776 Schwannoma**  
*Bryson Borg, MD and Kevin R. Moore, MD*

**780 Meningioma**  
*Bryson Borg, MD and Jeffrey S. Ross, MD*

**786 Solitary Fibrous Tumor/Hemangiopericytoma**  
*Bryson Borg, MD and Jeffrey S. Ross, MD*

**790 Neurofibroma**  
*Bryson Borg, MD and Kevin R. Moore, MD*

**794 Malignant Nerve Sheath Tumors**  
*Bryson Borg, MD and Jeffrey S. Ross, MD*

**798 Metastases, CSF Disseminated**  
*Bryson Borg, MD*

**802 Paraganglioma**  
*Bryson Borg, MD*

## INTRAMEDULLARY

**806 Astrocytoma**  
*Lubdha M. Shah, MD and Kevin R. Moore, MD*

**810 Cellular Ependymoma**  
*Kevin R. Moore, MD*

**814 Myxopapillary Ependymoma**  
*Kevin R. Moore, MD*

**818 Hemangioblastoma**  
*Lubdha M. Shah, MD and Jeffrey S. Ross, MD*

**824 Spinal Cord Metastases**  
*Lubdha M. Shah, MD and Jeffrey S. Ross, MD*

**828 Primary Melanocytic Neoplasms/Melanocytoma**  
*Lubdha M. Shah, MD and Jeffrey S. Ross, MD*

**830 Ganglioglioma**  
*Lubdha M. Shah, MD and Jeffrey S. Ross, MD*

## SECTION 2: NONNEOPLASTIC CYSTS AND TUMOR MIMICS

### CYSTS

**834 CSF Flow Artifact**  
*Lubdha M. Shah, MD and Kevin R. Moore, MD*

**836 Meningeal Cyst**  
*Lubdha M. Shah, MD and Jeffrey S. Ross, MD*

**842 Perineural Root Sleeve Cyst**  
*Kevin R. Moore, MD*

**846 Syringomyelia**  
*Kevin R. Moore, MD*

### NONNEOPLASTIC MASSES AND TUMOR MIMICS

**850 Epidural Lipomatosis**  
*Julia Crim, MD*

**852 Normal Fatty Marrow Variants**  
*Julia Crim, MD*

**854 Fibrous Dysplasia**  
*Julia Crim, MD*

**856 Kümmell Disease**  
*Julia Crim, MD and Kevin R. Moore, MD*

**858 Hirayama Disease**  
*Jeffrey S. Ross, MD*

**860 IgG4-Related Disease/Hypertrophic Pachymeningitis**  
*Jeffrey S. Ross, MD*

## SECTION 3: VASCULAR AND SYSTEMIC DISORDERS

### VASCULAR LESIONS

**866 Vascular Anatomy**  
*Jeffrey S. Ross, MD*

**872 Persistent First Intersegmental Artery**  
*Jeffrey S. Ross, MD*

**874 Persistent Hypoglossal Artery**  
*Jeffrey S. Ross, MD*

**876 Persistent Proatlantal Artery**  
*Jeffrey S. Ross, MD*

**878 Type 1 Vascular Malformation (dAVF)**  
*Jeffrey S. Ross, MD*

**884 Type 2 Arteriovenous Malformation (AVM)**  
*Jeffrey S. Ross, MD*

**888 Type 3 Arteriovenous Malformation (AVM)**  
*Jeffrey S. Ross, MD*

**892 Type 4 Vascular Malformation (AVF)**  
*Jeffrey S. Ross, MD*

**896 Conus Arteriovenous Malformation**  
*Jeffrey S. Ross, MD*

**900 Posterior Fossa Dural Fistula With Intraspinal Drainage**  
*Jeffrey S. Ross, MD*

**904 Cavernous Malformation**  
*Jeffrey S. Ross, MD*

**908 Spinal Artery Aneurysm**  
*Jeffrey S. Ross, MD*

**910 Spinal Cord Infarction**  
*Jeffrey S. Ross, MD*

**914 Subarachnoid Hemorrhage**  
*Jeffrey S. Ross, MD*

**918 Spontaneous Epidural Hematoma**  
*Jeffrey S. Ross, MD*

**924 Subdural Hematoma**  
*Jeffrey S. Ross, MD*

**928 Superficial Siderosis**  
*Jeffrey S. Ross, MD*

**932 Hematomyelia/Nontraumatic Cord Hemorrhage**  
*Jeffrey S. Ross, MD*

**936 Bow Hunter Syndrome**  
*Jeffrey S. Ross, MD*

**938 Vertebral Artery Dissection**  
*Lubdha M. Shah, MD*

### SPINAL MANIFESTATIONS OF SYSTEMIC DISEASES

**944 Osteoporosis**  
*Lubdha M. Shah, MD and Jeffrey S. Ross, MD*

**948 Paget Disease**  
*Lubdha M. Shah, MD*

# TABLE OF CONTENTS

- 952 **Hyperparathyroidism**  
*Julia Crim, MD*
- 954 **Renal Osteodystrophy**  
*Julia Crim, MD and Jeffrey S. Ross, MD*
- 956 **Hyperplastic Vertebral Marrow**  
*Lubdha M. Shah, MD and Jeffrey S. Ross, MD*
- 960 **Myelofibrosis**  
*Julia Crim, MD and Jeffrey S. Ross, MD*
- 962 **Bone Infarction**  
*Jeffrey S. Ross, MD*
- 964 **Extramedullary Hematopoiesis**  
*Lubdha M. Shah, MD*
- 968 **Tumoral Calcinosis**  
*Lubdha M. Shah, MD and Jeffrey S. Ross, MD*

## Part VI: Peripheral Nerve and Plexus

### SECTION 1: PLEXUS AND PERIPHERAL NERVE LESIONS

- 974 **Normal Plexus and Nerve Anatomy**  
*Kevin R. Moore, MD*
- 980 **Superior Sulcus Tumor**  
*Kevin R. Moore, MD*
- 984 **Thoracic Outlet Syndrome**  
*Kevin R. Moore, MD*
- 988 **Muscle Denervation**  
*Julia Crim, MD*
- 990 **Brachial Plexus Traction Injury**  
*Kevin R. Moore, MD*
- 994 **Idiopathic Brachial Plexus Neuritis**  
*Julia Crim, MD and Kevin R. Moore, MD*
- 998 **Traumatic Neuroma**  
*Julia Crim, MD and Kevin R. Moore, MD*
- 1002 **Radiation Plexopathy**  
*Kevin R. Moore, MD*
- 1006 **Peripheral Nerve Sheath Tumor**  
*Julia Crim, MD and Kevin R. Moore, MD*
- 1010 **Peripheral Neurolymphomatosis**  
*Kevin R. Moore, MD*
- 1012 **Hypertrophic Neuropathy**  
*Kevin R. Moore, MD*
- 1016 **Femoral Neuropathy**  
*Kevin R. Moore, MD*
- 1018 **Ulnar Neuropathy**  
*Kevin R. Moore, MD*
- 1022 **Suprascapular Neuropathy**  
*Julia Crim, MD*
- 1026 **Median Neuropathy**  
*Kevin R. Moore, MD*
- 1028 **Common Peroneal Neuropathy**  
*Kevin R. Moore, MD*
- 1030 **Tibial Neuropathy**  
*Julia Crim, MD*

## Part VII: Spine Postprocedural Imaging

### SECTION 1: POSTOPERATIVE IMAGING AND COMPLICATIONS

- 1036 **Surgical Approaches**  
*Jeffrey S. Ross, MD*
- 1040 **Normal Postoperative Change**  
*Bryson Borg, MD and Jeffrey S. Ross, MD*
- 1046 **Postoperative Spinal Complications**  
*Bryson Borg, MD and Jeffrey S. Ross, MD*
- 1052 **Myelography Complications**  
*Bryson Borg, MD and Jeffrey S. Ross, MD*
- 1056 **Vertebroplasty Complications**  
*Bryson Borg, MD and Jeffrey S. Ross, MD*
- 1060 **Failed Back Surgery Syndrome**  
*Jeffrey S. Ross, MD*
- 1064 **Recurrent Disc Herniation**  
*Jeffrey S. Ross, MD*
- 1068 **Peridural Fibrosis**  
*Jeffrey S. Ross, MD*
- 1072 **Arachnoiditis/Adhesions**  
*Bryson Borg, MD and Jeffrey S. Ross, MD*
- 1078 **Arachnoiditis Ossificans**  
*Bryson Borg, MD*
- 1080 **Accelerated Degeneration**  
*Jeffrey S. Ross, MD*
- 1084 **Postoperative Infection**  
*Lubdha M. Shah, MD and Jeffrey S. Ross, MD*
- 1088 **Pseudomeningocele**  
*Jeffrey S. Ross, MD*
- 1094 **CSF Leakage Syndrome**  
*Bryson Borg, MD*
- 1100 **Postsurgical Deformity**  
*Jeffrey S. Ross, MD*

### SECTION 2: HARDWARE

- 1106 **Metal Artifact**  
*Lubdha M. Shah, MD and Jeffrey S. Ross, MD*
- 1110 **Occipitocervical Fixation**  
*Lubdha M. Shah, MD and Jeffrey S. Ross, MD*
- 1112 **Plates and Screws**  
*Lubdha M. Shah, MD and Jeffrey S. Ross, MD*
- 1116 **Cages**  
*Lubdha M. Shah, MD*
- 1118 **Interbody Fusion Devices**  
*Lubdha M. Shah, MD and Jeffrey S. Ross, MD*
- 1122 **Interspinous Spacing Devices**  
*Lubdha M. Shah, MD and Jeffrey S. Ross, MD*
- 1126 **Cervical Artificial Disc**  
*Lubdha M. Shah, MD and Jeffrey S. Ross, MD*
- 1130 **Lumbar Artificial Disc**  
*Lubdha M. Shah, MD and Jeffrey S. Ross, MD*
- 1134 **Hardware Failure**  
*Jeffrey S. Ross, MD and Lubdha M. Shah, MD*
- 1140 **Bone Graft Complications**  
*Jeffrey S. Ross, MD*



# TABLE OF CONTENTS

**1144 rhBMP-2 Complications**

*Jeffrey S. Ross, MD*

**1148 Heterotopic Bone Formation**

*Jeffrey S. Ross, MD*

## SECTION 3: POST RADIATION AND CHEMOTHERAPY COMPLICATIONS

**1154 Radiation Myelopathy**

*Kevin R. Moore, MD*

**1158 Post-Irradiation Vertebral Marrow**

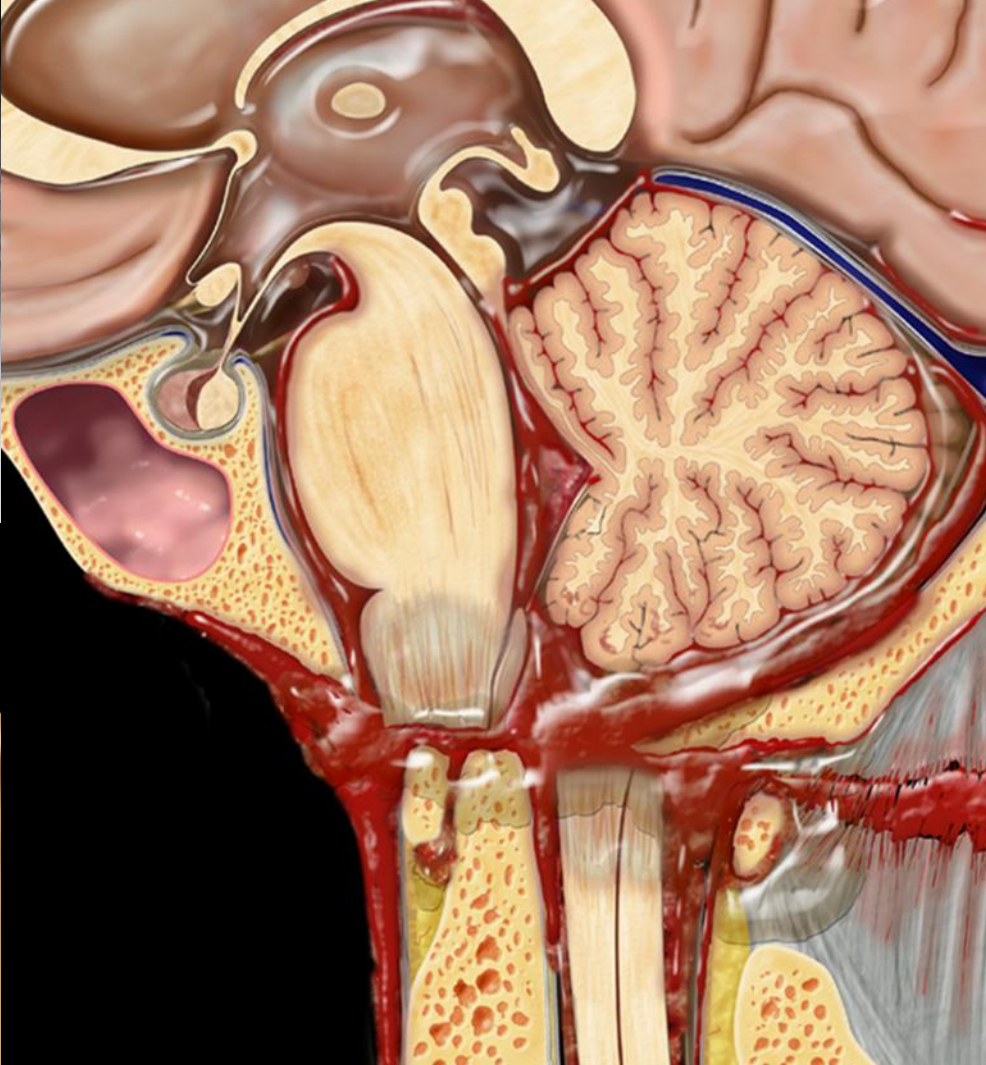
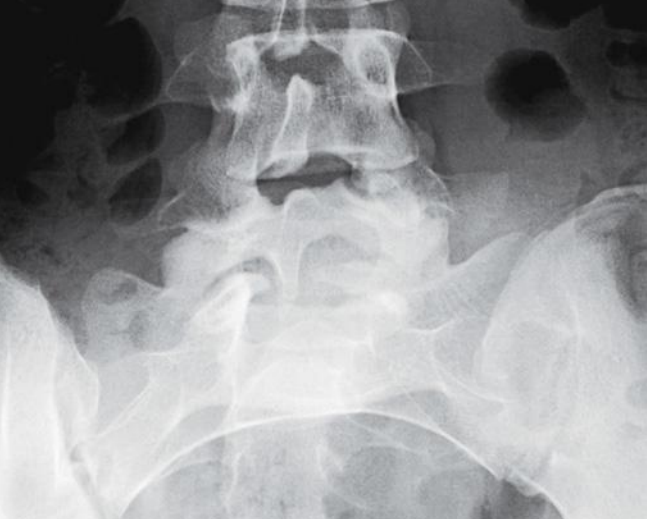
*Kevin R. Moore, MD*

**1162 Anterior Lumbar Radiculopathy**

*Kevin R. Moore, MD*

This page intentionally left blank

This page intentionally left blank

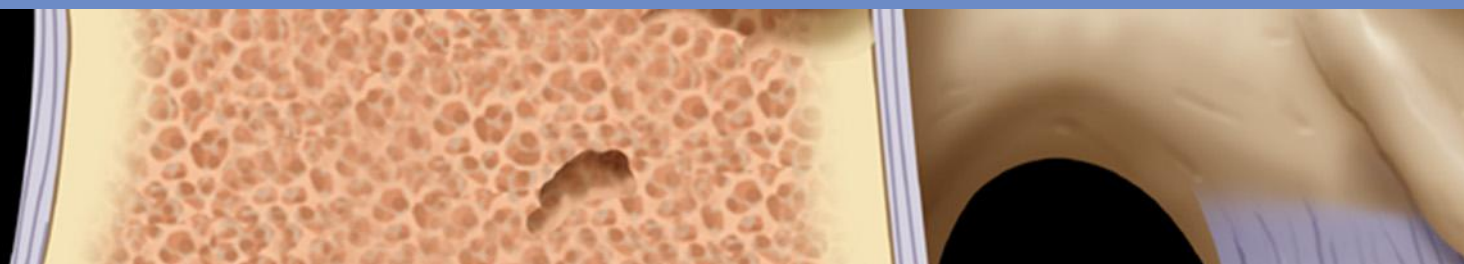


*Diagnostic Imaging*

# Spine



PART I  
SECTION 1  
Congenital



**Normal Anatomical Variations**

Normal Anatomy	4
Measurement Techniques	10
MR Artifacts	16
Normal Variant	22
Craniovertebral Junction Variants	26
Ponticulus Posticus	30
Ossiculum Terminale	32
Conjoined Nerve Roots	34
Limbus Vertebra	38
Filum Terminale Fibrolipoma	42
Bone Island	44
Ventriculus Terminalis	46

**Chiari Disorders**

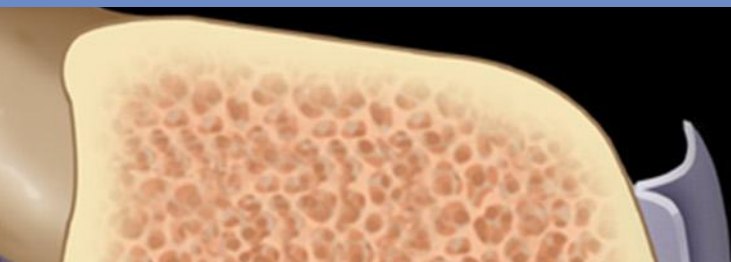
Chiari 0	50
Chiari 1	52
Complex Chiari	56
Chiari 2	58
Chiari 3	62

**Abnormalities of Neurulation**

Approach to Spine and Spinal Cord Development	64
Myelomeningocele	72
Lipomyelomeningocele	76
Lipoma	80
Dorsal Dermal Sinus	84
Simple Coccygeal Dimple	88
Dermoid Cysts	92
Epidermoid Cysts	96

**Anomalies of the Caudal Cell Mass**

Tethered Spinal Cord	100
Segmental Spinal Dysgenesis	104
Caudal Regression Syndrome	108
Terminal Myelocystocele	112



Anterior Sacral Meningocele	116
Sacral Extradural Arachnoid Cyst	120
Sacrococcygeal Teratoma	124

### **Anomalies of Notochord and Vertebral Formation**

Craniovertebral Junction Embryology	128
Paracondylar Process	132
Split Atlas	134
Klippel-Feil Spectrum	136
Failure of Vertebral Formation	140
Vertebral Segmentation Failure	144
Diastematomyelia	148
Partial Vertebral Duplication	152
Incomplete Fusion, Posterior Element	154
Neurenteric Cyst	156

### **Developmental Abnormalities**

Os Odontoideum	160
Lateral Meningocele	164
Dorsal Spinal Meningocele	168
Dural Dysplasia	172

### **Genetic Disorders**

Neurofibromatosis Type 1	176
Neurofibromatosis Type 2	180
Achondroplasia	186
Mucopolysaccharidoses	190
Sickle Cell Disease	194
Osteogenesis Imperfecta	198
Tuberous Sclerosis	202
Osteopetrosis	206
Gaucher Disease	208
Ochronosis	210
Connective Tissue Disorders	212
Spondyloepiphyseal Dysplasia	216
Thanatophoric Dwarfism	220

## Imaging Anatomy

There are **33** spinal vertebrae, which comprise two components: A cylindrical ventral bone mass, which is the vertebral **body**, and the dorsal **arch**.

### 7 cervical, 12 thoracic, 5 lumbar bodies

- 5 fused elements form the sacrum
- 4-5 irregular ossicles form the coccyx

### Arch

- 2 pedicles, 2 laminae, 7 processes (1 spinous, 4 articular, 2 transverse)
- Pedicles attach to the dorsolateral aspect of the body
- Pedicles unite with a pair of arched flat laminae
- Lamina capped by dorsal projection called the spinous process
- Transverse processes arise from the sides of the arches

The two articular processes (zygapophyses) are diarthrodial joints.

- (1) Superior process bearing a facet with the surface directed dorsally
- (2) Inferior process bearing a facet with the surface directed ventrally

**Pars interarticularis** is the part of the arch that lies between the superior and inferior articular facets of all subatlantal movable elements. The pars are positioned to receive biomechanical stresses of translational forces displacing superior facets ventrally, whereas inferior facets remain attached to dorsal arch (spondylolysis). C2 exhibits a unique anterior relation between the superior facet and the posteriorly placed inferior facet. This relationship leads to an elongated C2 pars interarticularis, which is the site of the hangman's fracture.

### Cervical

The cervical bodies are small and thin relative to the size of the arch and foramen, with the transverse diameter greater than the AP diameter. The lateral edges of the superior surface of the body are turned upward into the uncinat processes. The transverse foramen perforates the transverse processes. The vertebral artery resides within the transverse foramen, most commonly starting at the C6 level.

C1 has no body and forms a circular bony mass. The superior facets of C1 are large ovals that face upwards and the inferior facets are circular in shape. Large transverse processes are present on C1 with fused anterior and posterior tubercles.

The C2 complex consists of the axis body with dens/odontoid process. The odontoid embryologically arises from the centrum of the first cervical vertebrae.

The C7 vertebral body shows a transitional morphology with a prominent spinous process.

### Thoracic

- Thoracic bodies are heart-shaped and increase in size from superior to inferior
- Facets are present for rib articulation and the laminae are broad and thick
- Spinous processes are long, directed obliquely caudally
- Superior facets are thin and directed posteriorly
- The T1 vertebral body shows a complete facet for the capitulum of the first rib, and an inferior demifacet for capitulum of second rib

- The T12 body has transitional anatomy, and resembles the upper lumbar bodies with the inferior facet directed more laterally

### Lumbar

The lumbar vertebral bodies are large, wide and thick, and lack a transverse foramen or costal articular facets. The pedicles are strong and directed posteriorly. The superior articular processes are directed dorsomedially and almost face each other. The inferior articular processes are directed anteriorly and laterally.

### Joints

**Synarthrosis** is an immovable joint of cartilage, and occurs during development and in the first decade of life. The neurocentral joint occurs at the union point of two centers of ossification for two halves of the vertebral arch and centrum.

**Diarthrosis** is a true synovial joint that occurs in the articular processes, costovertebral joints, and atlantoaxial and sacroiliac articulations. The pivot-type joint occurs at the median atlantoaxial articulation. All others are gliding joints.

**Amphiarthroses** are nonsynovial, movable connective tissue joints. **Symphysis** is a fibrocartilage fusion between two bones, as in the intervertebral disc. **Syndesmosis** is a ligamentous connection common in the spine, such as the paired ligamenta flava, intertransverse ligaments, and interspinous ligaments. An unpaired syndesmosis is present in the supraspinous ligament.

**Atlantooccipital** articulation is composed of a diarthrosis between the lateral mass of atlas and occipital condyles and the syndesmoses of the atlantooccipital membranes. Anterior AO membrane is the extension of the ALL. The posterior AO membrane is homologous to the ligamenta flava.

**Atlantoaxial** articulation is a pivot joint. The transverse ligament maintains the relationship of the odontoid to the anterior arch of atlas. Synovial cavities are present between the transverse ligament/odontoid and the atlas/odontoid junctions.

### Disc

The intervertebral disc is composed of three parts: The **cartilaginous endplate**, the **anulus fibrosus**, and the **nucleus pulposus**. The height of the lumbar disc space generally increases as one progresses caudally. The anulus consists of concentrically oriented collagenous fibers which serve to contain the central nucleus pulposus. These fibers insert into the vertebral cortex via Sharpey fibers and also attach to the anterior and posterior longitudinal ligaments. Type I collagen predominates at periphery of anulus, while type II collagen predominates in the inner anulus. The normal contour of the posterior aspect of the anulus is dependent upon the contour of its adjacent endplate. Typically, this is slightly concave in the axial plane; although, commonly at L4-L5 and L5-S1 these posterior margins will be flat or even convex. A convex shape on the axial images alone should not be interpreted as degenerative bulging.

The nucleus pulposus is a remnant of the embryonal notochord and consists of a well-hydrated, noncompressible proteoglycan matrix with scattered chondrocytes. Proteoglycans form a major macromolecular component, including chondroitin 6-sulfate, keratan sulfate, and hyaluronic acid. Proteoglycans consist of protein core with multiple attached glycosaminoglycan chains. The nucleus occupies an

eccentric position within the confines of anulus and is more dorsal with respect to the center of the vertebral body. At birth, approximately 85-90% of the nucleus is water. This water content gradually decreases with advancing age. Within the nucleus pulposus on T2-weighted sagittal images, there is often a linear hypointensity coursing in an anteroposterior direction, the intranuclear cleft. This region of more prominent fibrous tissue should not be interpreted as intradiscal air or calcification.

### Anterior Longitudinal Ligament (ALL)

The ALL runs along the ventral surface of the spine from the skull to the sacrum. The ALL is narrowest in the cervical spine and is firmly attached at the ends of each vertebral body. It is loosely attached at the midsection of the disc.

### Posterior Longitudinal Ligament (PLL)

The PLL runs on the dorsal surface of bodies from the skull to the sacrum. The PLL has a segmental denticulate configuration and is wider at the disc space, but narrows and becomes thicker at the vertebral body level.

### Craniocervical Ligaments

The craniocervical ligaments are located anteriorly to spinal cord and occur in three layers: Anterior, middle, and posterior. Anterior ligaments consist of the odontoid ligaments (apical and alar). The apical ligament is a small fibrous band extending from dens tip to basion. Alar ligaments are thick, horizontally directed ligaments extending from the lateral surface of dens tip to anteromedial occipital condyles. The middle layer consists of the cruciate ligament. The **transverse ligament** is a strong horizontal component of the cruciate ligament extending from behind the dens to the medial aspect of C1 lateral masses. The craniocaudal component consists of a fibrous band running from the transverse ligament superiorly to the foramen magnum and inferiorly to C2. Posteriorly, the tectorial membrane is the continuation of PLL and attaches to anterior rim of the foramen magnum.

### Vertebral Artery

The vertebral artery arises as the first branch of the subclavian artery on both sides. The vertebral artery travels cephalad within the foramen transversarium (transverse foramen) within the transverse processes. The first segment of the vertebral artery extends from its origin to the entrance into the foramen of the transverse process of the cervical vertebrae, usually the 6th. The most common variation is the origin of the left vertebral from the arch, between the left common carotid and the left subclavian arteries (2-6%). The vertebral artery in these variant cases almost always enters the foramen of the transverse process of C5. The second segment runs within the transverse foramen to the C2 level. Nerve roots pass posterior to the vertebral artery. The third segment starts at the C2 level where the artery loops and turns lateral to ascend in the C1 transverse foramen. It then turns medial crossing on top of C1 in a groove. The fourth segment starts where the artery perforates the dura and arachnoid at lateral edge of posterior occipitoatlantal membrane, coursing ventrally on the medulla to join with the other vertebral to make the basilar artery.

### Vertebral Column Blood Supply

Paired segmental arteries (intercostals, lumbar arteries) arise from the aorta and extend dorsolaterally around the middle of the vertebral body. Near the transverse process the

segmental artery divides into lateral and dorsal branches. The lateral branch supplies dorsal musculature and the dorsal branch passes lateral to the foramen, giving off branch(es) and providing major vascular supply to bone and vertebral canal contents. The posterior central branch supplies disc and vertebral body, while the prelaminar branch supplies the inner surface of the arch, ligamenta flava, and regional epidural tissue. The neural branch entering the neural foramen supplies pia, arachnoid, and cord. The postlaminar branch supplies musculature overlying lamina and branches to bone.

### Nerves

- Spinal nerves are arranged in 31 pairs and grouped regionally: 8 cervical, 12 thoracic, 5 lumbar, 5 sacral, 1 coccygeal
- Ascensus spinalis is the apparent developmental rising of the cord related to differential spinal growth
- Course of nerve roots becomes longer and more oblique at lower segments
- C1 nerve from C1 segment and exits above C1
- C8 nerve from C7 segment and exits at C7-T1
- T6 nerve from T5 segment and exits at T6-T7
- T12 nerve from T8 segment and exits at T12-L1
- L2 nerve from T10 segment and exits at L2-L3
- S3 nerve from T12 segment and exits at the S3 foramen

**Meninges** are divided into dura, arachnoid, and pia

**Dura** is a dense, tough covering corresponding to the meningeal layer of the cranial dura. The epidural space is filled with fat, loose connective tissue, and veins. The dura continues with spinal nerves through the foramen to fuse with the epineurium. Cephalic attachment of the dura is at the foramen magnum and the caudal attachment at the back of the coccyx.

**Arachnoid** is the middle covering, which is thin, delicate, and continuous with cranial arachnoid. The arachnoid is separated from the dura by the potential subdural space.

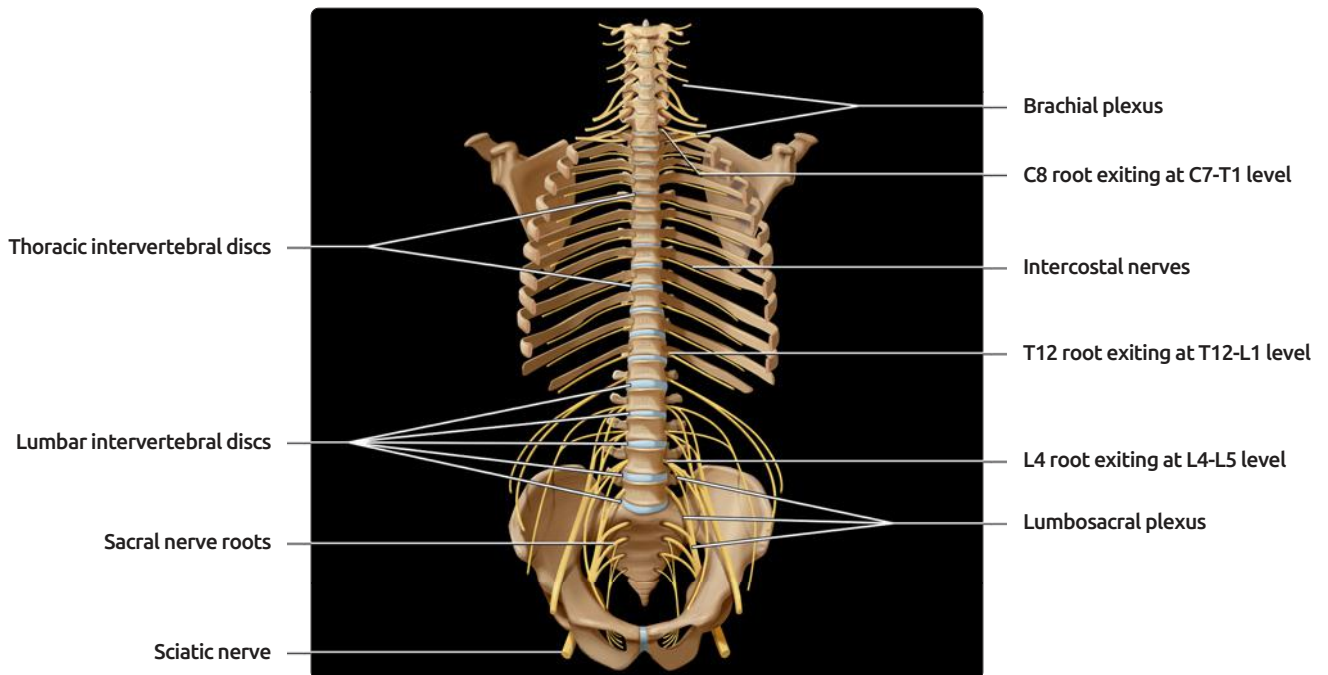
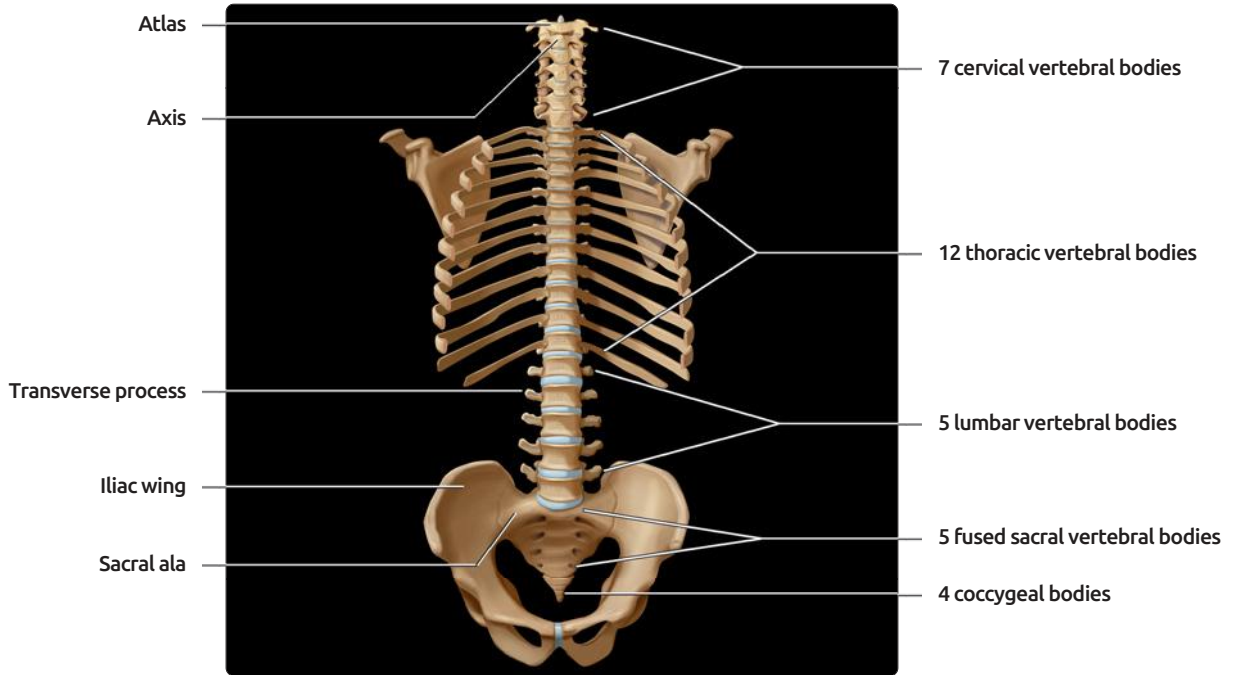
**Pia** is the inner covering of delicate connective tissue closely applied to the cord. Longitudinal fibers are laterally concentrated as denticulate ligaments lying between posterior and anterior roots, and attach at 21 points to dura. Longitudinal fibers are concentrated dorsally as the septum posticum attaching the dorsal cord to the dorsal midline dura.

### Selected References

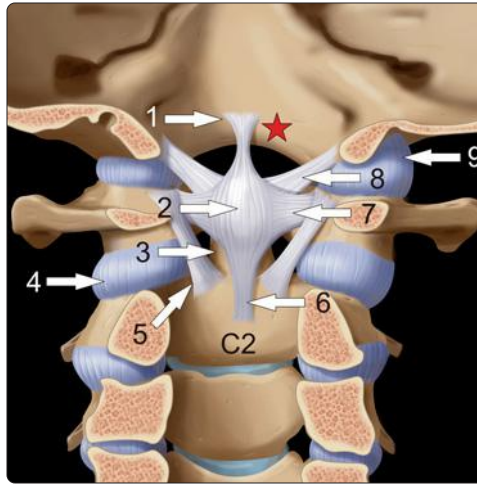
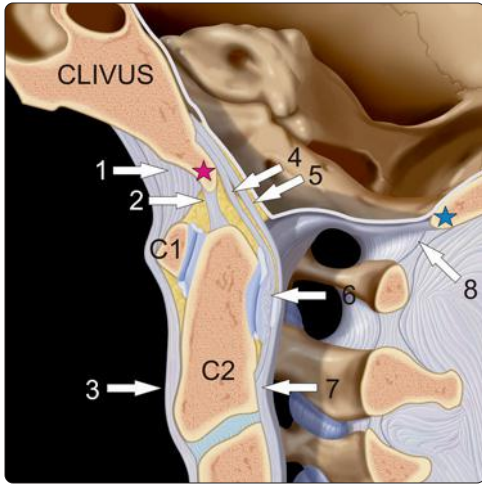
1. Griessenauer CJ et al: Venous drainage of the spine and spinal cord: A comprehensive review of its history, embryology, anatomy, physiology, and pathology. *Clin Anat.* 28(1):75-87, 2015
2. Fardon DF et al: Lumbar disc nomenclature: version 2.0: recommendations of the combined task forces of the north american spine society, the american society of spine radiology, and the american society of neuroradiology. *Spine (Phila Pa 1976).* 39(24):E1448-65, 2014
3. Santillan A et al: Vascular anatomy of the spinal cord. *J Neurointerv Surg.* 4(1):67-74, 2012
4. Modic MT et al: Lumbar degenerative disk disease. *Radiology.* 245(1):43-61, 2007
5. Battie MC et al: Lumbar disc degeneration: epidemiology and genetics. *J Bone Joint Surg Am.* 88 Suppl 2:3-9, 2006
6. Grunhagen T et al: Nutrient supply and intervertebral disc metabolism. *J Bone Joint Surg Am.* 88 Suppl 2:30-5, 2006
7. Haughton V: Imaging intervertebral disc degeneration. *J Bone Joint Surg Am.* 88 Suppl 2:15-20, 2006
8. Roh JS et al: Degenerative disorders of the lumbar and cervical spine. *Orthop Clin North Am.* 36(3):255-62, 2005



# Normal Anatomy



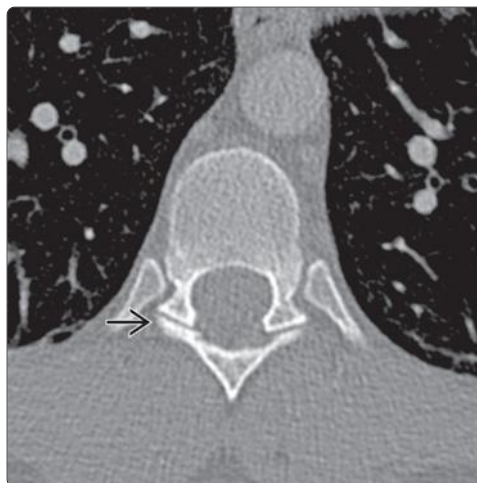
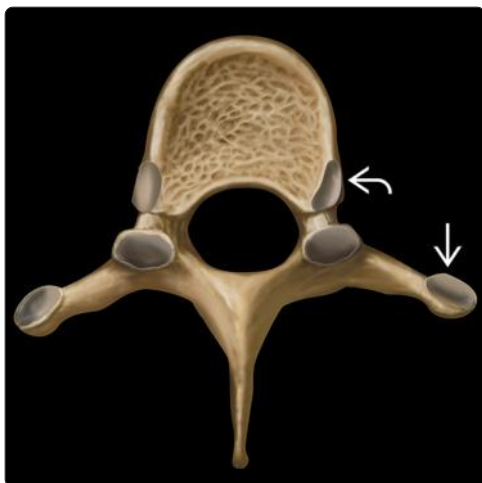
**(Top)** Coronal graphic of the spinal column shows relationship of 7 cervical, 12 thoracic, 5 lumbar, 5 fused sacral, and 4 coccygeal bodies. Note cervical bodies are smaller with neural foramina oriented at 45° and capped by the unique C1 and C2 morphology. Thoracic bodies are heart-shaped, with thinner intervertebral discs, and are stabilized by the rib cage. Lumbar bodies are more massive, with prominent transverse processes and thick intervertebral discs. **(Bottom)** Coronal graphic demonstrates exiting spinal nerve roots. C1 exits between the occiput and C1, while the C8 root exits at the C7-T1 level. Thoracic and lumbar roots exit below their respective pedicles.



(Left) Sagittal graphic of CVJ shows: 1) Ant. atlantooccipital membrane, 2) apical lig., 3) ALL, 4) cruciate lig., 5) tectorial membrane, 6) transverse lig., 7) post. longitudinal lig., and 8) post. atlantooccipital membrane. Red star is the basion; blue star is the opisthion. (Right) Posterior view of CVJ shows: 1) Sup. cruciate ligament, 2) cruciate lig., 3) odontoid ant. to cruciate lig., 4) atlantoaxial jt., 5) accessory atlantoaxial lig., 6) inf. cruciate lig., 7) transverse lig., 8) alar lig., and 9) atlantooccipital jt. Red star = basion.



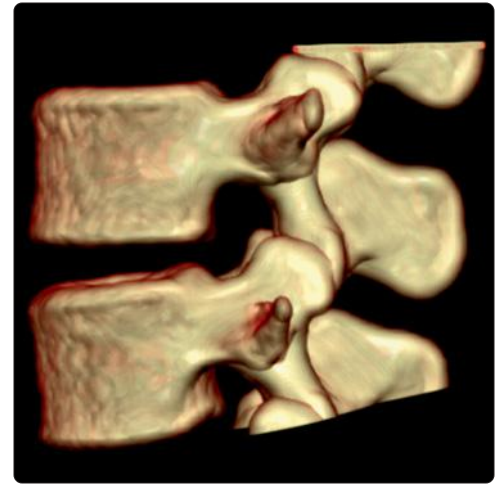
(Left) Graphic shows cervical vertebra from above. Vertebral body is broad transversely, central canal is large and triangular in shape, pedicles are directed posterolaterally, and laminae are delicate. Lateral masses contain the vertebral foramen for passage of vertebral artery and veins. (Right) Mid-C5 body at the pedicle level: Transverse foramina are prominent  $\Rightarrow$ , encompassing the vertical course of vertebral artery. The anterior and posterior tubercles  $\Rightarrow$  give rise to muscle attachments in neck.



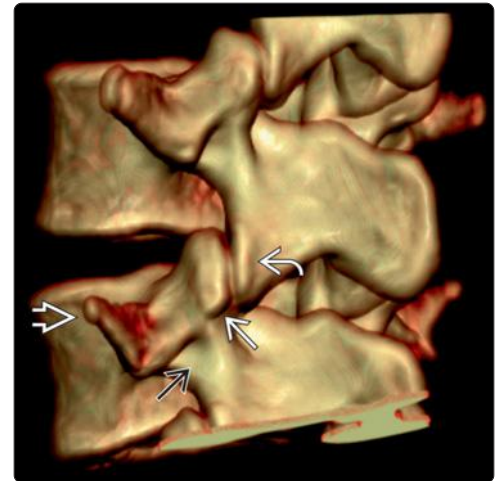
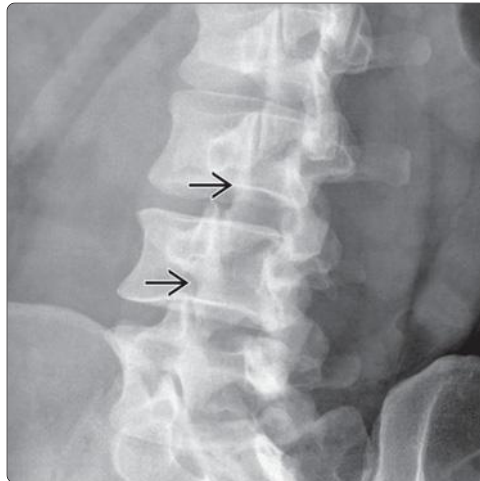
(Left) Graphic shows thoracic vertebral body from above. Thoracic bodies are characterized by long, spinous processes and transverse processes. Complex rib articulation includes both costotransverse joints  $\Rightarrow$  and costovertebral joints  $\Rightarrow$ . Facet joints are oriented in the coronal plane. (Right) Image through the pedicle level of the thoracic spine: The coronal orientation of the facet joints are well identified in this section  $\Rightarrow$ . The pedicles are thin and gracile, with adjacent rib articulations.

# Normal Anatomy

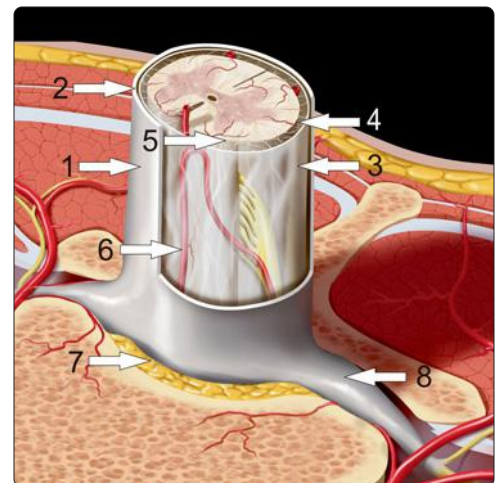
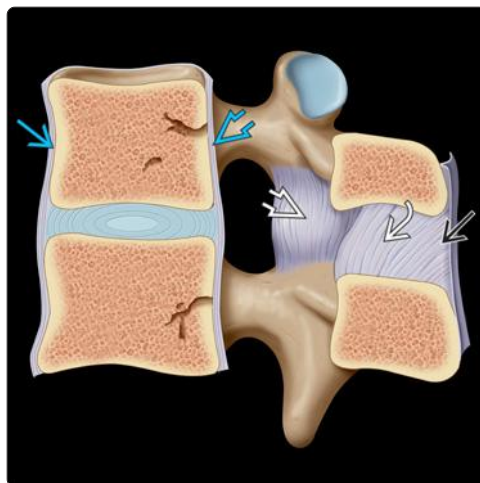
(Left) Graphic shows lumbar body from above. Large, sturdy lumbar bodies connect to thick pedicles and transversely directed transverse processes. Facets maintain oblique orientation favoring flexion/extension. (Right) Lateral 3D scan of the lumbar spine shows large bodies joined by thick posterior elements with the superior and inferior articular processes angled in lateral plane. Transverse processes jut out laterally for muscle attachments. Pars interarticularis form a junction between articular processes.



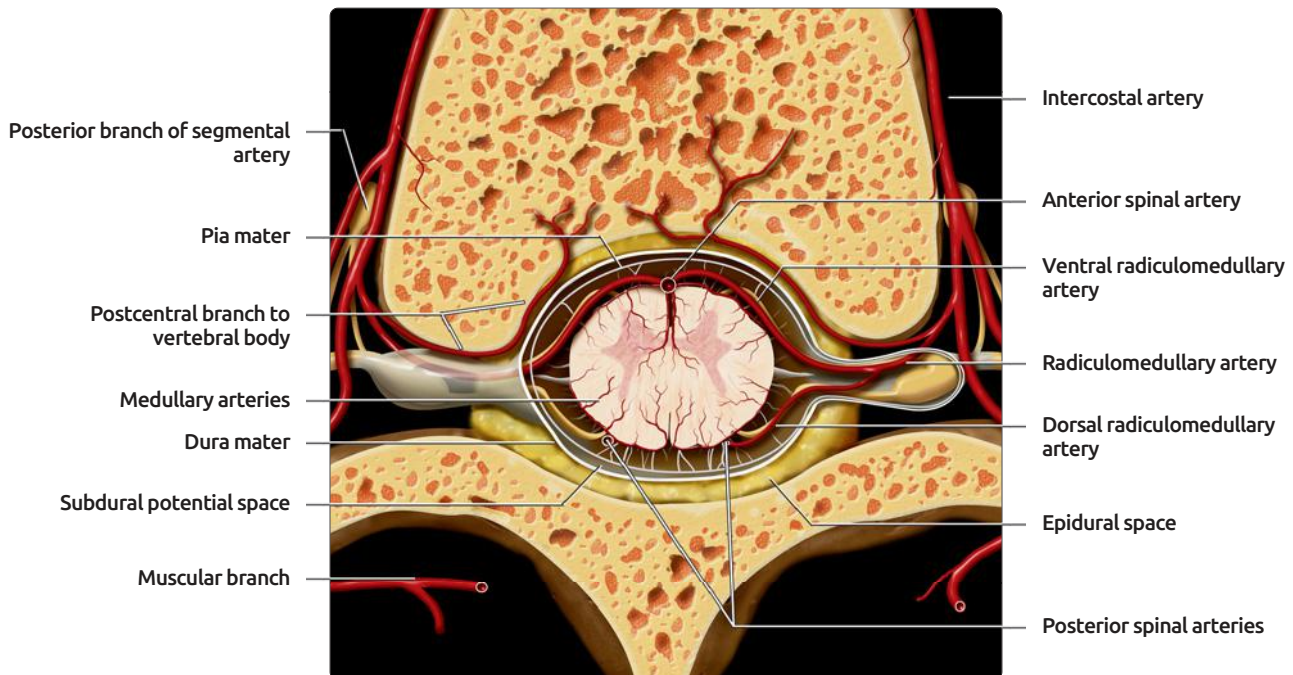
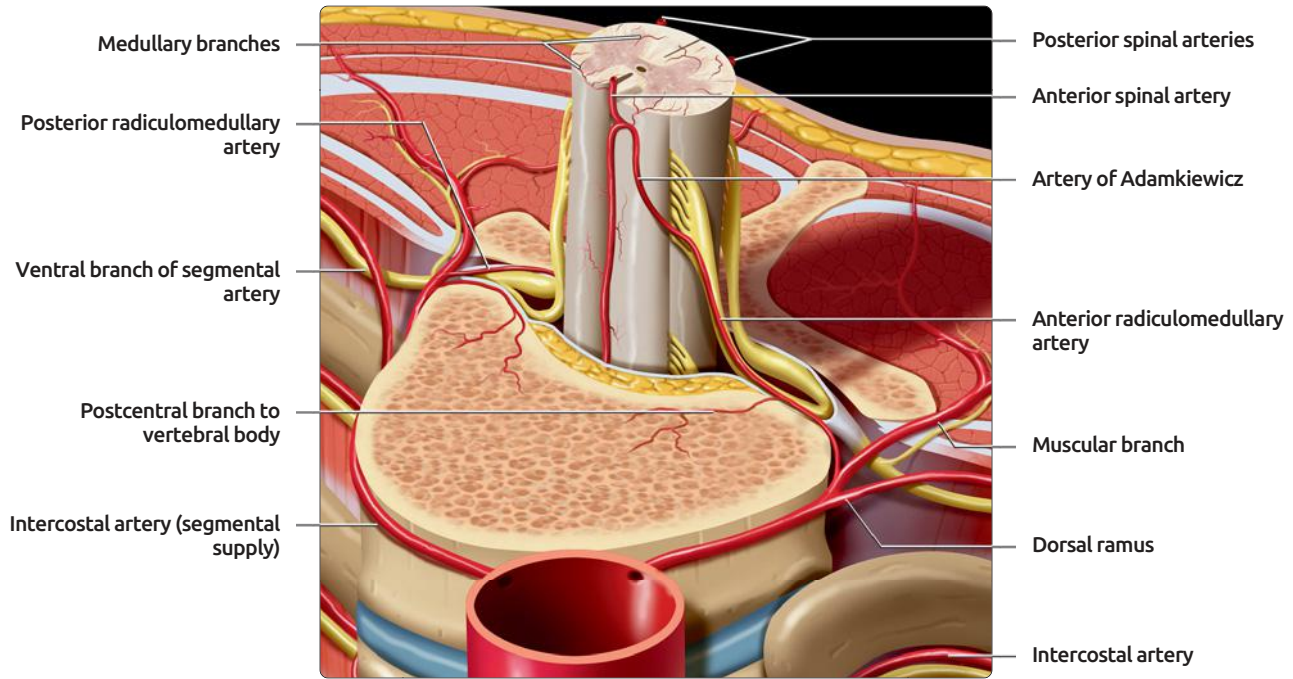
(Left) Coronal oblique view of the lumbar spine shows the typical "scotty dog" appearance of the posterior elements. The neck of the "dog" is the pars interarticularis. (Right) Oblique 3D exam of lumbar spine shows surface anatomy of "scotty dog": Transverse process (nose), superior articular process (ear), inferior articular process (front leg), and intervening pars interarticularis (neck). Pedicle that forms "eye" on CT reconstructions is obscured.



(Left) Cut-away graphic shows lumbar vertebral bodies joined by disc & anterior & posterior longitudinal ligaments. Paired ligamentum flavum & interspinous ligament join posterior elements, with midline supraspinous ligament. (Right) Graphic shows spinal cord and coverings: 1) dura mater, 2) subdural space, 3) arachnoid mater, 4) subarachnoid space, 5) pia mater, 6) ant. spinal artery, 7) epidural space, and 8) root sleeve.







**(Top)** Oblique axial graphic of the thoracic spinal cord and arterial supply at T10 shows segmental intercostal arteries arising from the lower thoracic aorta. The artery of Adamkiewicz is the dominant segmental feeding vessel to the thoracic cord, supplying the anterior aspect of the cord via the anterior spinal artery. Adamkiewicz has a characteristic "hairpin" turn on the cord surface as it first courses superiorly, then turns inferiorly. **(Bottom)** Axial graphic shows the anterior and posterior radiculomedullary arteries anastomosing with the anterior and posterior spinal arteries. Penetrating medullary arteries in the cord are largely end-arteries with few collaterals. The cord "watershed" zone is at the central gray matter.

## Terminology

Radiographic measurement techniques, skull base craniometry, skull base lines

## Pathology-Based Imaging Issues

This chapter provides a broad summary of the varied measurement techniques used for evaluating the spine. The main focus for the reader should be the tables and the multiple schematics that define the variously named lines and angles. These summarize the classic measurement techniques for the skull base, rheumatoid disease, and some of the most commonly used measurements for assessing trauma. The rest of the measurements defined below are a mixture of miscellaneous measurements and those that do not translate well into a table (i.e., equations).

### Torg-Pavlov Ratio

- Diameter of canal to width of vertebral body (initially defined on plain radiographs of the subaxial spine)

The practical utility of this measurement is controversial. Less than 0.80 as seen on the lateral view is considered to be cervical stenosis, and such a small canal potentially increases risk for cord injury.

### Maximum Canal Compromise (%)

- $= 1 - (Di / ((Da + Db) / 2)) \times 100\%$

AP canal diameter at the normal levels (immediately above and below the level of injury) and at the level of maximum compromise are defined. The measurement of normal levels is taken at the midvertebral body level. **Di** is the anteroposterior canal diameter at the level of maximum injury, **Da** is the AP canal diameter at the nearest normal level above the level of injury, and **Db** is the AP canal diameter at the nearest normal level below the level of injury.

In spinal cord injury patients, midline T1 and T2 images provide an objective, quantifiable, and reliable assessment of cord compression that cannot be defined by CT alone.

### Maximum Cord Compression (%)

- $= 1 - (di / ((da + db) / 2)) \times 100\%$

AP cord diameter at the normal levels immediately above and below the level of injury and at the level of maximum cord compression is defined. **di** is the anteroposterior cord diameter at the level of maximum injury, **da** is the AP cord diameter at the nearest normal level above the level of injury, and **db** is the AP cord diameter at the nearest normal level below the level of injury. If cord edema is present, then measurements are made at the midvertebral body level just above or below the extent of the edema where cord appears normal.

### Cobb Measurement of Kyphosis

Lines are drawn to mark the superior endplate of the superior next unaffected vertebral body and the inferior endplate of the inferior next unaffected vertebral body, which are then extended anterior to the bony canal. Perpendicular lines are then extended and the angle between the 2 perpendicular lines is measured.

### Tangent Method for Kyphosis

Lines are drawn along the posterior vertebral body margin on the lateral view of the affected body and the next most superior body that is unaffected. The angle between these 2 vertically oriented lines is measured.

## Centroid

Also called the geometric center of the vertebral body, this measurement is defined by drawing diagonal lines between opposite corners of the body, with the centroid at the intersection.

### Apical Vertebral Translation (AVT)

Lateral displacement of the apex of the coronal curve is relative to the **center sacral vertical line** (CSVL) on AP plain film. The AVT is the horizontal distance between the centroid of the apical body and the CSVL.

### Sagittal Balance

Sagittal alignment is defined on the lateral view using a C7 plumb line. The distal reference point is the posterior superior aspect of the sacrum. There is a positive number if C7 plumb line falls anterior to the reference point, and a negative number if it falls posterior to the reference.

## Selected References

1. Andreisek G et al: Consensus conference on core radiological parameters to describe lumbar stenosis - an initiative for structured reporting. *Eur Radiol.* 24(12):3224-32, 2014
2. Karpova A et al: Reliability of quantitative magnetic resonance imaging methods in the assessment of spinal canal stenosis and cord compression in cervical myelopathy. *Spine (Phila Pa 1976).* 38(3):245-52, 2013
3. Radcliff KE et al: Comprehensive computed tomography assessment of the upper cervical anatomy: what is normal? *Spine J.* 10(3):219-29, 2010
4. Rojas CA et al: Evaluation of the C1-C2 articulation on MDCT in healthy children and young adults. *AJR Am J Roentgenol.* 193(5):1388-92, 2009
5. Angevine PD et al: Radiographic measurement techniques. *Neurosurgery.* 63(3 Suppl):40-5, 2008
6. Bono CM et al: Measurement techniques for upper cervical spine injuries: consensus statement of the Spine Trauma Study Group. *Spine (Phila Pa 1976).* 32(5):593-600, 2007
7. Furlan JC et al: A quantitative and reproducible method to assess cord compression and canal stenosis after cervical spine trauma: a study of interrater and intrarater reliability. *Spine (Phila Pa 1976).* 32(19):2083-91, 2007
8. Pang D et al: Atlanto-occipital dislocation—part 2: The clinical use of (occipital) condyle-C1 interval, comparison with other diagnostic methods, and the manifestation, management, and outcome of atlanto-occipital dislocation in children. *Neurosurgery.* 61(5):995-1015; discussion 1015, 2007
9. Pang D et al: Atlanto-occipital dislocation: part 1—normal occipital condyle-C1 interval in 89 children. *Neurosurgery.* 61(3):514-21; discussion 521, 2007
10. Bono CM et al: Measurement techniques for lower cervical spine injuries: consensus statement of the Spine Trauma Study Group. *Spine (Phila Pa 1976).* 31(5):603-9, 2006
11. Fehlings MG et al: The optimal radiologic method for assessing spinal canal compromise and cord compression in patients with cervical spinal cord injury. Part II: Results of a multicenter study. *Spine (Phila Pa 1976).* 24(6):605-13, 1999
12. Rao SC et al: The optimal radiologic method for assessing spinal canal compromise and cord compression in patients with cervical spinal cord injury. Part I: An evidence-based analysis of the published literature. *Spine (Phila Pa 1976).* 24(6):598-604, 1999
13. Harris JH Jr et al: Radiologic diagnosis of traumatic occipitovertebral dissociation: 1. Normal occipitovertebral relationships on lateral radiographs of supine subjects. *AJR Am J Roentgenol.* 162(4):881-6, 1994
14. Harris JH Jr et al: Radiologic diagnosis of traumatic occipitovertebral dissociation: 2. Comparison of three methods of detecting occipitovertebral relationships on lateral radiographs of supine subjects. *AJR Am J Roentgenol.* 162(4):887-92, 1994
15. Powers B et al: Traumatic anterior atlanto-occipital dislocation. *Neurosurgery.* 4(1):12-7, 1979



## Common CV Junction Measurements

Measurement	Definition	Normal	Abnormal
<b>Chamberlain (palatooccipital) line</b>	Posterior hard palate to opisthion	< 2.5 mm of dens above line	Dens > 2.5 mm above line
<b>McGregor (basal) line</b>	Posterior hard palate to lowest point of occipital bone	Tip of dens < 4.5 mm above line	Tip of dens > 4.5 mm above line
<b>McRae line</b>	Basion to opisthion	Entire dens below line	< 19 mm
<b>Wackenheim clival line</b>	Dorsum sellae to tip of clivus	Entire dens ventral to line	Dens bisects line
<b>Fischgold digastric line</b>	Connects the 2 digastric fossae	Entire dens below line	Dens bisects line
<b>Fischgold bimaistoid line</b>	Connects tips of mastoid processes	Tip of dens 3 mm below to 10 mm above line	Tip of dens > 10 mm above line
<b>Anterior atlantodental interval</b>	Posterior aspect of anterior C1 arch to anterior margin odontoid process	Plain films in children: < 4-5 mm; plain film in adults: Males < 3.0 mm, females < 2.5 mm; sagittal CT reformats in children: < 2.6 mm; sagittal CT in adults: Both males and females < 2.0 mm	Plain films in children: > 4-5 mm; plain film in adults: Males > 3.0 mm, females > 2.5 mm; sagittal CT reformats in children: > 2.6 mm; sagittal CT in adults: Both males and females > 2.0 mm
<b>Atlantooccipital joint space</b>	Line from midpoint of occipital condyle to C1 condylar fossa	Plain films in children: < 5 mm; CT in children: < 2.5 mm	Plain films in children: > 5 mm; CT in children: > 2.5 mm
<b>Summed condylar distance</b>	Sum of bilateral distances between midpoint of occipital condyle and C1 condylar fossa	CT in adults: < 4.2 mm	
<b>Atlantoaxial joint space</b>	Line defining midpoint of C1-C2 joint on coronal view	CT in adults: < 3.4 mm; CT in children: < 3.9 mm	CT in adults: > 3.4 mm; CT in children: > 3.9 mm

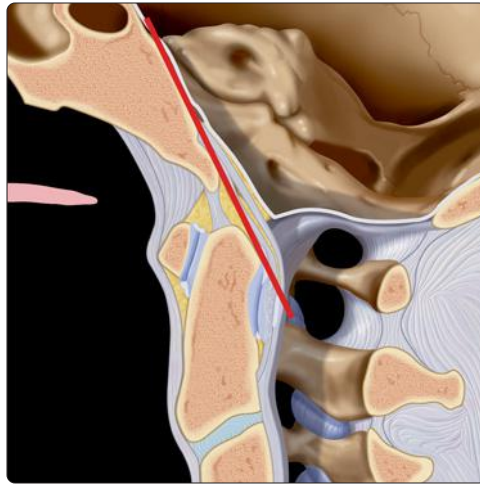
## Rheumatoid Arthritis Measurements

Measurement	Definition	Normal	Abnormal
<b>Ranawat</b>	Distance between center of C2 pedicle and transverse axis of atlas measured along axis of odontoid process	< 15 mm in males, < 13 mm in females	≥ 15 mm in males, ≥ 13 mm in females
<b>Redlund-Johnell line</b>	Distance between McGregor line and midpoint of caudal margin C2	< 34 mm in males, < 29 mm in females	≥ 34 mm in males, ≥ 29 mm in females
<b>Clark stations</b>	Dividing odontoid process into 3 parts in sagittal plane	Anterior ring of atlas is level with 1st station	Anterior ring of atlas is level with middle 1/3 (2nd station) or caudal 1/3 (3rd station)
<b>Posterior atlantodental interval (PADI)</b>	Horizontal distance from posterior dens to anterior aspect of C1 lamina or ring		Smaller is worse and relates to potential neurologic deficit
<b>Space available for cord (SAC)</b>	AP diameter on sagittal MR study between dorsal and ventral dura	> 13 mm	SAC < 13 mm then decompression in RA patients considered
<b>Spinal canal diameter (SCD)</b>	Horizontal measurement from posterior vertebral body to spinolaminar line		On plain films < 14 mm, canal stenosis warrants MR for further evaluation

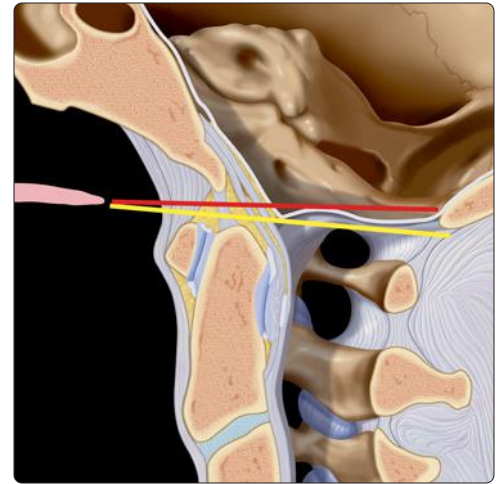
## CV Junction Trauma Measurements

Measurement	Definition	Normal	Abnormal
<b>Basion dental interval (BDI)</b>	Basion to superior aspect of odontoid process	< 12-12.5 mm in children on plain films, < 10.5 mm in children by sagittal CT, < 8.5 mm in adults	> 12 mm (Harris measurement)
<b>Basion axial interval (BAI)</b>	Distance between basion and a line drawn along posterior cortical margin of C2	0-12 mm on plain films	Highly variable and not recommended as primary diagnostic method
<b>Powers ratio</b>	Ratio of distance between basion and C1 posterior arch divided by distance between opisthion and midpoint of posterior aspect of anterior C1 arch (BC/OA)	< 1.0	> 1.0 (anterior dislocation only) posterior dissociation or vertical distraction could be missed with normal value

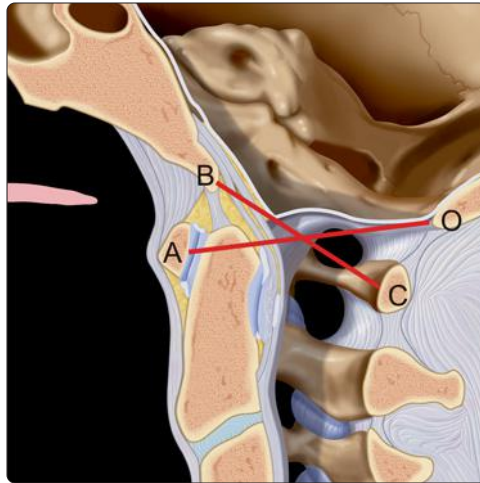
**(Left)** Sagittal graphic of craniocervical junction shows Wackenheim clival line (red) extending tangent to the normal odontoid position. The line is drawn from the dorsum sellae to the tip of clivus.



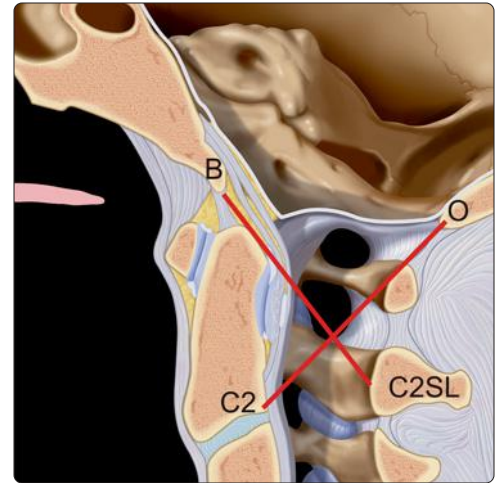
**(Right)** Sagittal graphic of the craniocervical junction shows Chamberlain line (red), drawn from the posterior hard palate to opisthion, and McGregor line (yellow), drawn from the posterior hard palate to the lowest point of the occipital bone.



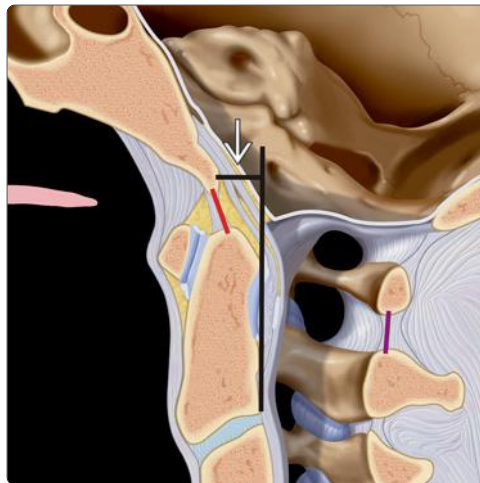
**(Left)** Sagittal graphic of craniocervical junction shows lines comprising the Powers ratio (BC/OA), where normal is < 1. BC = basion to C1 posterior arch, OA = opisthion and midpoint of the posterior aspect of anterior C1 arch.



**(Right)** Sagittal graphic shows lines comprising the Lee method. BC2SL and C2O should just intersect tangentially with the posterosuperior aspect of the dens and the highest point on the atlas spinolaminar line respectively in normal state. Deviation suggests AOD.

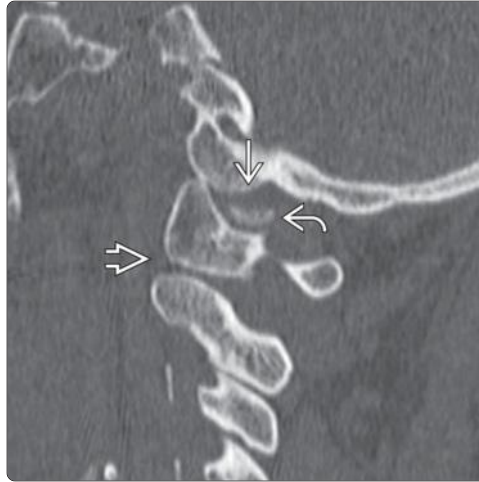


**(Left)** Sagittal graphic shows basion dental interval (BDI) in red, which should be < 12-12.5 mm in children on plain films and < 8.5 mm in adults on CT. Black lines define basion axial interval (BAI) extending from basion to line extended along posterior margin of C2, which should be < 12 mm on plain films. C1-C2 spinolaminar line is shown in purple (< 8 mm in adults).



**(Right)** Sagittal graphic shows atlantodental interval (green) and spinal canal diameter (red).

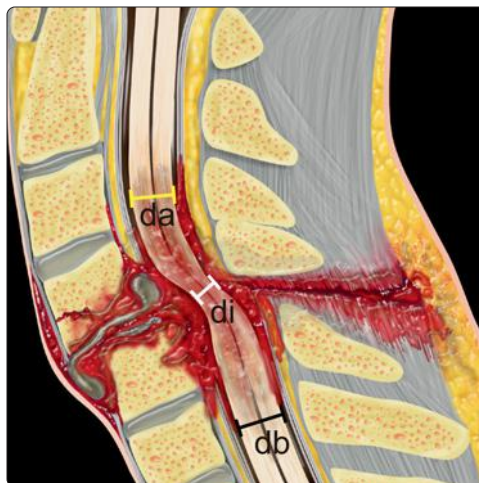
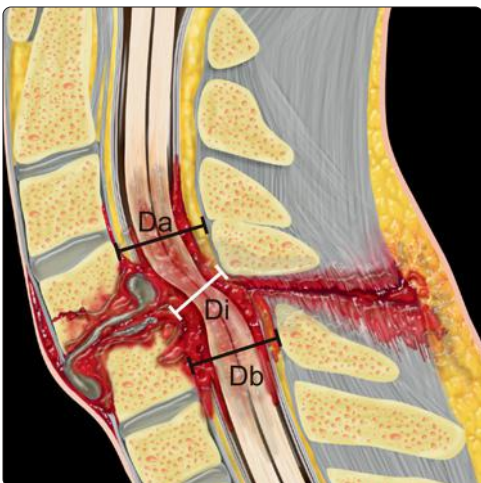




(Left) Sagittal CT reconstruction in AOD shows widening of the BDI  $> 8.5$  mm in this adult. Note the normal Wackenheim line relationship. (Right) Sagittal CT reconstruction in AOD shows widening of the C0-C1 junction with anterior subluxation of the condyle. Condylar fragment is present in the joint space. Note the normal C1-C2 relationship.



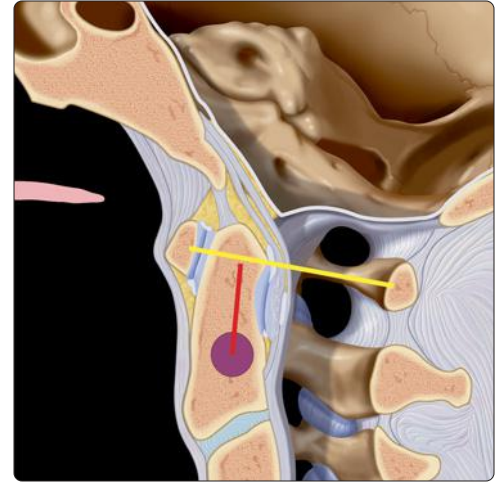
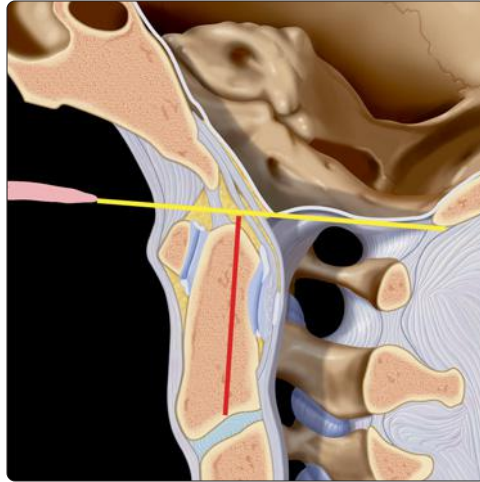
(Left) Sagittal STIR MR in AOD shows widening of BDI with  $\uparrow$  T2 signal from alar and apical ligament rupture. Note also prevertebral edema and posterior interspinous ligament disruption. Posterior epidural hemorrhage contributes to subarachnoid space narrowing. (Right) Coronal CT reconstruction in AOD shows marked widening of the C0-C1 joint space, which should be approximately 2 mm. Bilateral symmetric avulsion fractures off of the condyles are present.



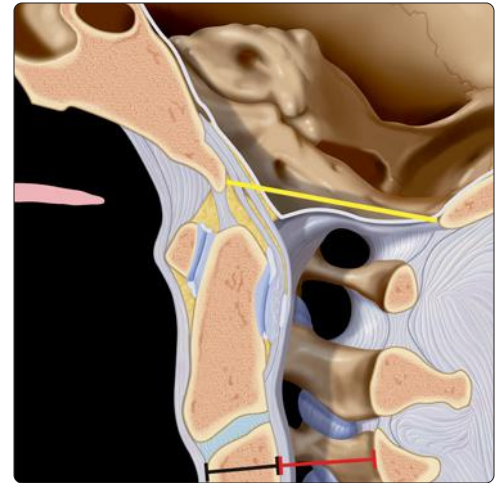
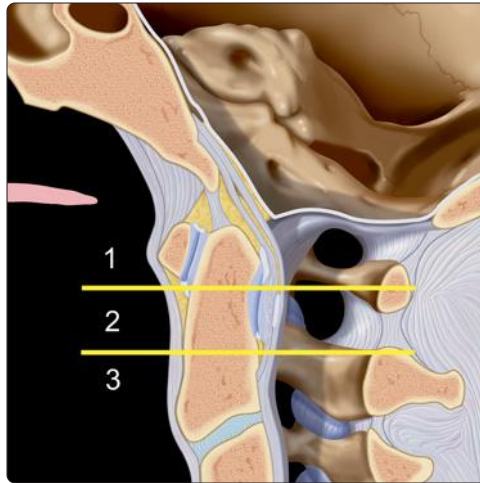
(Left) Sagittal graphic shows the maximum canal compromise measurement. Di is the anteroposterior canal diameter at the level of maximum injury, Da is the AP canal diameter at the nearest normal level above the level of injury. Db is AP canal diameter at nearest normal level below level of injury. (Right) Sagittal graphic shows maximum cord compression measurement. di is AP cord diameter at level of maximum injury. da is AP cord diameter at nearest normal level above injury. db is AP cord diameter at nearest normal level below injury.



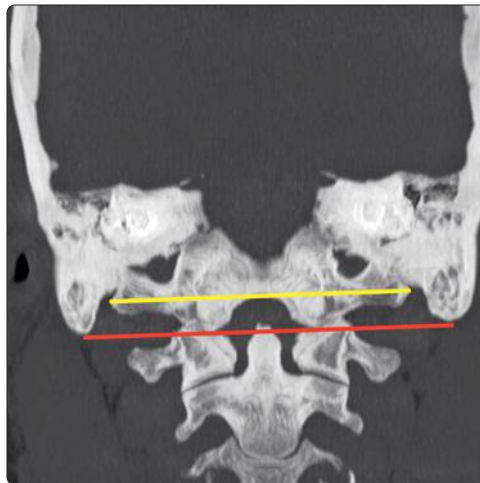
(Left) Sagittal graphic shows Redlund-Johnell line (red) defined by distance between McGregor line (yellow) and midpoint of caudal margin of C2 body. (Right) Sagittal graphic shows Ranawat measurement as the distance between the center of C2 pedicle (purple) and transverse axis (yellow) of the atlas measured along the axis of the odontoid process.

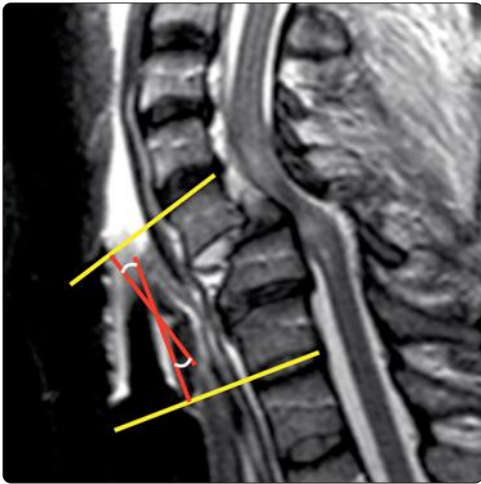


(Left) Graphic shows the 3 Clarke stations for measuring basilar impression in RA. If anterior ring of C1 is level with the 2nd or 3rd station, then basilar impression is present. (Right) Sagittal graphic shows 2 different measurements: McRae line (yellow) is defined from basion to opisthion, and the dens should be below this line. Length of McRae should be > 19 mm. Lower measurement shows measurements of Torg-Pavlov ratio, which is the diameter of canal (red) to width of vertebral body (black). Normal is > 0.8.

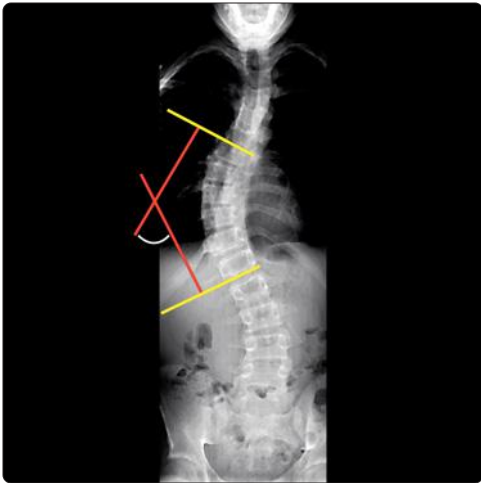


(Left) Coronal CT shows Fischgold digastric line (yellow) connecting the 2 digastric fossae (normal when dens below the line), and Fischgold bimastoid line (red) connecting the mastoid processes (abnormal if tip of dens > 10 mm above line). (Right) Sagittal CT shows upward translocation of odontoid with Wackenheim clival line and Chamberlain line grossly abnormal in this patient with RA. Odontoid is eroded with thinned pencil-tip appearance. Note markedly increased atlantodental interval.

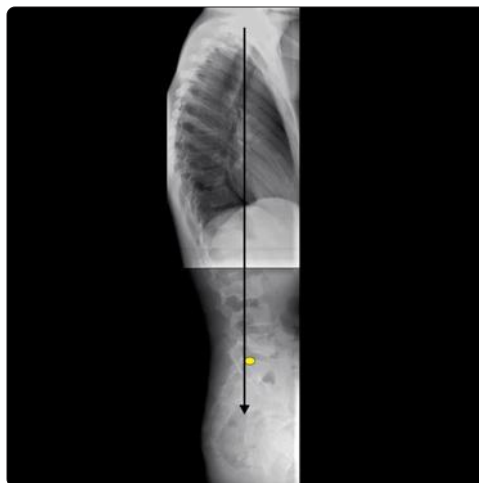




(Left) Sagittal graphic shows Cobb angle method for cervical kyphosis. Lines are drawn along superior endplate of cephalad unaffected body and inferior endplate of caudal unaffected body (yellow). The angle of perpendiculars (red) from these lines is considered Cobb angle (white). (Right) Sagittal graphic shows posterior vertebral body tangent method. Lines extend from the posterior body at fractured level and superior unaffected level. Distance can be measured (red) or angle of lines determined.



(Left) AP view shows Cobb measurement. Lines are drawn (yellow) along end vertebrae, which are upper and lower limits of curve tilting most severely toward concavity. Perpendiculars are drawn from the endplate lines (red), with angle measurement (white). (Right) Anteroposterior radiograph shows measurement of overall coronal plane balance by the distance (yellow) from C7 plumb line (white) to central sacral vertical line (CSVL) (black). Positive displacement is to the right, negative to the left.



(Left) Anteroposterior radiograph shows measurement of apical vertebral translation (AVT). Distance (arrowed line) from centroid of apex of curve (yellow) is measured relative to CSVL (black). (Right) Lateral radiograph shows measurement of sagittal balance. Horizontal displacement measured from plumb line extended from centroid of C7 (black line) to posterior superior margin of the sacrum (yellow). Positive balance when line is anterior to reference point.



## KEY FACTS

### TERMINOLOGY

- MR imaging artifacts that simulate disease

### IMAGING

- Artfactual "pseudolesion" is usually bizarre or nonanatomic in appearance or distribution
  - May be detected anywhere in spine
- Common artifacts
  - Truncation ("Gibbs") artifact
  - Phase ghosting artifact
  - Motion artifact
  - CSF flow artifact
  - Chemical shift artifact
  - Wraparound artifact (aliasing)
  - Susceptibility artifact
  - Zipper artifact
  - Gradient warping artifact
  - Fat-saturation failure ± inappropriate water saturation

- Normal marrow T1 hypointensity at high field strength ( $\geq 3.0$  tesla)

### TOP DIFFERENTIAL DIAGNOSES

- Syringohydromyelia
- CSF drop metastases
- Aneurysm or arteriovenous malformation
- Spinal cord hemorrhage
- Marrow infiltration or replacement

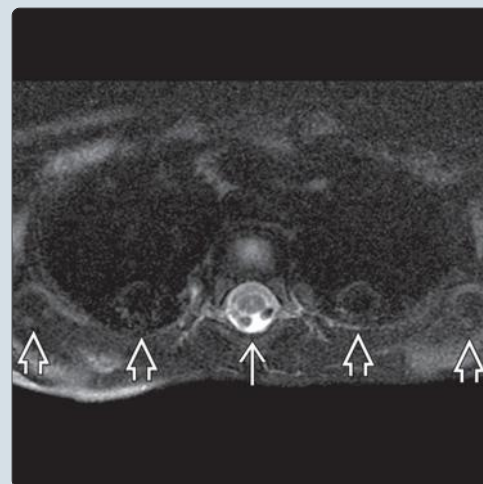
### CLINICAL ISSUES

- Artifact location often unrelated to clinical findings

### DIAGNOSTIC CHECKLIST

- Always consider MR artifacts when confronted with bizarre imaging findings

**(Left)** Sagittal STIR MR demonstrates linear T2 hyperintensity within the lower thoracic spinal cord extending to the conus, representing motion artifact from abdominal wall movement. The appearance is suspicious for artifact, because it continues to the conus tip, unusual with true syringomyelia. **(Right)** Axial T2WI FS MR demonstrates prominent periodic ghosting artifact of the thecal sac propagated across the image in the phase direction.



**(Left)** Sagittal T2WI MR obtained for CSF drop metastasis surveillance shows bizarre intradural T2 hypointensity, representing marked CSF pulsation artifact in the thoracic spine. **(Right)** Axial T2WI MR (imaging surveillance for CSF drop metastases) confirms intradural low signal intensity CSF pulsation artifact. Correct interpretation as artifact is possible by recognizing that this low signal intensity does not resemble either a normal anatomic structure or typical drop metastasis.



**TERMINOLOGY****Abbreviations**

- Specific absorbed radiation (SAR), cerebrospinal fluid (CSF), radiofrequency (RF)

**Synonyms**

- "Phase ghosting," "Gibbs" artifact, "blooming" artifact

**Definitions**

- MR imaging artifacts that simulate disease

**IMAGING****General Features**

- Best diagnostic clue
  - Artifactual "pseudolesion" is usually bizarre or nonanatomic in appearance or distribution
- Location
  - May be detected anywhere in spine
    - Appearance depends on artifact type
- Size
  - Variable
- Morphology
  - Bizarre appearance that seems nonphysiological or nonanatomical
    - MR is very prone to imaging artifacts
    - Fortunately, most are pretty unique in appearance, readily identified if reader is aware of their existence
  - Compare with CT motion artifacts, which often simulate spine fractures or congenital anomalies on reformatted images

**MR Findings**

- Truncation ("Gibbs") artifact
  - Mathematical artifact related to truncation of computational series used during Fourier transformation of K-space data
    - Not possible to calculate infinite series when reconstructing raw data
    - Mathematical equation is "truncated" or shortened to reflect practical necessity of sampling finite, rather than infinite, number of frequencies
  - May be detected in both phase and encoding directions, although more conspicuous in phase direction, because fewer samples usually obtained
  - Occurs at high contrast interfaces, producing alternating light and dark bands that may mimic lesions
  - In spine, may artifactually widen or narrow spinal cord or mimic syrinx
  - Decrease artifact conspicuity by ↑ number of phase encoding steps or ↓ field of view (FOV)
- Phase ghosting artifact
  - Periodic replication of structure along line in phase encoding direction
  - Ghost artifacts, in particular, occur whenever there is periodic motion within field of view FOV
    - Examples include blood flow in vessels, CSF pulsations, cardiac, and respiratory motion
  - Like many artifacts, phase ghosting is more conspicuous in phase encoding direction, because sampling times are much slower than in frequency encoding direction

- Thus, these artifacts are propagated in phase direction regardless of motion direction
- Motion artifact
  - Voluntary or involuntary patient movement (random) or pulsating flow in vessels (periodic)
  - Detected in phase encoding direction
  - May simulate pathologic intramedullary or intradural lesion
    - Usually recognizable as artifact, but may render study limited or nondiagnostic for cord pathology
  - If motion is nonperiodic (e.g., bowel peristalsis), ghosting will not occur, but generalized image degradation will be apparent
  - Address with patient instruction, respiratory compensation, sedation, faster scanning
- CSF flow artifact
  - Subset of periodic motion artifact
  - Dephasing of protons due to CSF motion may simulate intradural blood, disc herniation, CSF metastasis, or intramedullary lesion
  - Flow compensation techniques can decrease artifact conspicuity
- Chemical shift artifact
  - Protons precess at slightly different frequencies in fat compared to water
    - Difference in proton precessional frequency between water and fat at 1.5T is 220 Hz
  - Spatial misregistration of fat and water produces overlap that causes additive bright band at lower frequency range and subtractive dark band at higher frequency range
  - Can be useful to confirm presence of macroscopic fat
- Wraparound artifact (aliasing)
  - Occurs when dimensions of imaged object exceed FOV
  - Seen in both frequency and phase encoding directions, although much more conspicuous in phase encoding direction
  - May also be identified in slice select direction on 3D sequences, because of additional phase encoding direction
  - Increasing FOV and number of phase encoding steps helps reduce artifact in phase direction, as does use of "no phase wrap" software
  - Aliasing in frequency direction may be abolished by oversampling above Nyquist frequency
- Susceptibility artifact
  - Metal or blood products disrupt local magnetic field homogeneity, produce signal void or image distortion
  - Common in postoperative instrumented spine
  - New metal-insensitive pulse sequences help reduce artifact
  - Can be used to advantage to diagnose hemorrhagic or calcified lesions
    - e.g., cavernous malformations, spinal cord hemorrhage
- Zipper artifact
  - Family of similar appearing artifacts most commonly occurring in phase encoding direction

- Produced by radiofrequency noise related to scanner equipment, scan parameters, or extrinsic noise (TV or radio channel, flickering fluorescent room light, patient monitor, etc.)
- Usually easy to identify as artifact, but may obscure important findings or create confusing pseudolesion
- Gradient warping artifact
  - Image distortion at edges of large FOV studies (> 30 cm) caused by gradient distortion
  - May be addressed with gradient distortion correction (GDC)
- Fat-saturation failure ± inappropriate water saturation
  - Frequency selective RF ("fat-saturation") pulse frequency chosen to saturate fat spectral peak center frequency
  - Magnetic field inhomogeneity alters fat center frequency so that fat-saturation pulse frequency no longer overlaps fat spectral peak → fat-saturation failure
  - If fat-saturation pulse frequency inadvertently overlaps water spectral peak → inappropriate water suppression
- Normal marrow T1 hypointensity at high field strength ( $\geq 3.0$  T)
  - Problem arises because of technical parameter changes needed to acquire T1-weighted images at high field in reasonable time without SAR issues
  - Inversion recovery T1WI sequences less SAR intensive than T1 SE sequence, commonly used in 3.0T spine imaging
    - Marrow signal relatively hypointense compared to appearance on SE T1WI, simulates pathological marrow infiltration

### Imaging Recommendations

- Protocol advice
  - Minimize artifacts using appropriate parameters, flow compensation, saturation bands, adequate sedation, or comfort measures, etc.

## DIFFERENTIAL DIAGNOSIS

### Syringomyelia

- True dilation of central spinal cord canal, without (hydromyelia) or with (syringomyelia) underlying cord injury and myelomalacia, eccentric cavitation
- Does not usually extend all the way to conus; may be sacculated
- Simulated by truncation artifact or phase ghosting

### CSF Drop Metastases

- Will usually be detectable in at least 2 planes
- Mimicked (or obscured) by CSF pulsation artifact
- Swap phase and frequency if needed to confirm as not an artifact

### Aneurysm or Arteriovenous Malformation

- Phase ghosting permits diagnosis of patent flow within vessels or tissue based on periodic ghost artifact
- Absence of this artifact in technically satisfactory MR exam indicates slow flow or thrombosed lesion

### Spinal Cord Hemorrhage

- Cavernous malformation, post-traumatic spinal cord hematoma, neoplasm
- Mimicked by phase ghosting, RF leak, motion artifact

- Use gradient recalled echo imaging (GRE) to capitalize on susceptibility artifact, confirm blooming of hypointense signal in hemorrhagic lesion

### Marrow Infiltration or Replacement

- Marrow replacement or ablation, fibrosis
- Hematopoietic neoplasms, marrow replacement, or ablation diseases, osteopetrosis
- Mimicked by use of T1 FLAIR technique for T1WI at higher field strengths ( $\geq 3.0$ T)
- Results in lower normal marrow signal intensity than seen on spin-echo T1WI sequences

## CLINICAL ISSUES

### Presentation

- Most common signs/symptoms
  - Artifact location often unrelated to clinical findings
  - Exception is susceptibility artifact in cases of hemorrhage, metallic foreign body, or medical devices

### Natural History & Prognosis

- Not applicable

### Treatment

- Not applicable

## DIAGNOSTIC CHECKLIST

### Consider

- Artifacts often have characteristic appearance, recognizable if imager is aware of and considers artifact

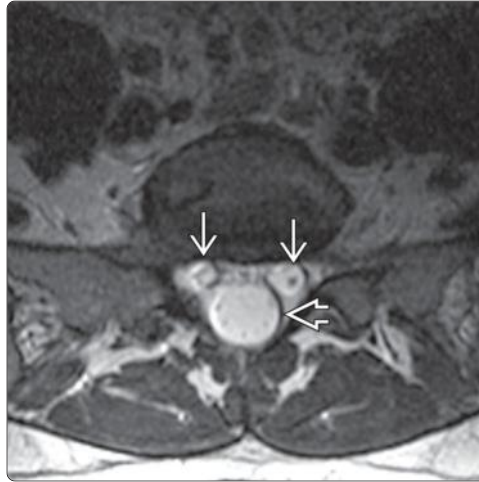
### Reporting Tips




- Always consider MR artifacts when confronted with bizarre imaging findings
  - If MR artifact cannot be excluded, consider true pathology
  - Clinical context always crucial to avoid failure to consider important pathologic differential considerations

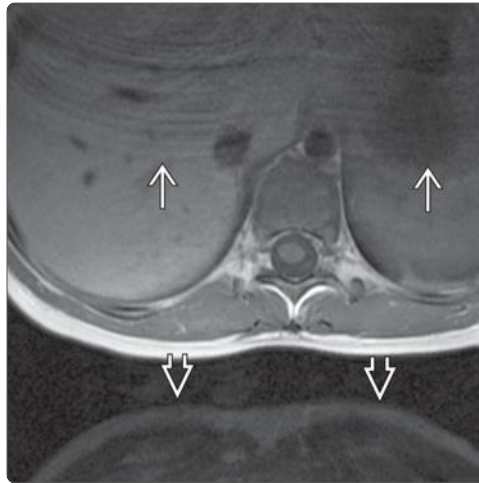
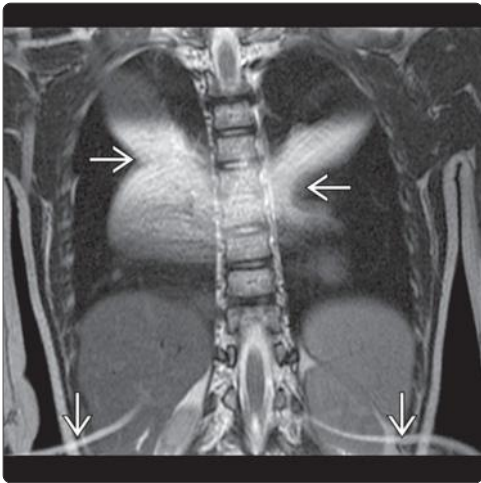
## SELECTED REFERENCES



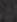
1. Zaitsev M et al: Motion artifacts in MRI: A complex problem with many partial solutions. *J Magn Reson Imaging*. ePub, 2015
2. Mohankumar R et al: Pitfalls and pearls in MRI of the knee. *AJR Am J Roentgenol*. 203(3):516-30, 2014
3. Motamedi D et al: Pitfalls in shoulder MRI: part 1—normal anatomy and anatomic variants. *AJR Am J Roentgenol*. 203(3):501-7, 2014
4. Motamedi D et al: Pitfalls in shoulder MRI: part 2—biceps tendon, bursae and cysts, incidental and postsurgical findings, and artifacts. *AJR Am J Roentgenol*. 203(3):508-15, 2014
5. Dagia C et al: 3T MRI in paediatrics: challenges and clinical applications. *Eur J Radiol*. 68(2):309-19, 2008
6. Fries P et al: Magnetic resonance imaging of the spine at 3 Tesla. *Semin Musculoskelet Radiol*. 12(3):238-52, 2008
7. Shapiro MD: MR imaging of the spine at 3T. *Magn Reson Imaging Clin N Am*. 14(1):97-108, 2006
8. Elster AD et al: Questions and Answers in Magnetic Resonance Imaging. St. Louis: Mosby. 123-47, 2001
9. Peh WC et al: Artifacts in musculoskeletal magnetic resonance imaging: identification and correction. *Skeletal Radiol*. 30(4):179-91, 2001

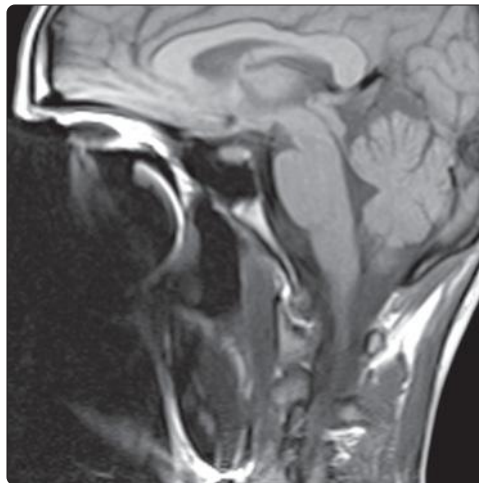






(Left) Axial T2WI MR in a patient with tethered spinal cord shows classic chemical shift artifact , confirming presence of fat within the filum. Pattern of alternating hyper- and hypointensity confirms that frequency direction is AP. (Right) Axial T2WI MR depicts prominent chemical shift artifact in the thecal sac  and nerve root sleeves  reflecting presence of water (CSF in root sleeves) and fat (epidural) within adjacent voxels. Frequency direction is right to left.

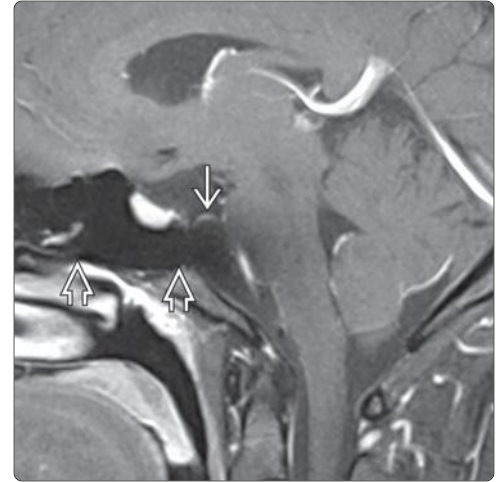




(Left) Coronal T2WI MR demonstrates artifactual wrap of back fat  onto the thoracic spine. Such artifacts could be diminished by increasing the field of view (FOV), at the cost of spatial resolution, unless the number of phase encoding steps is also increased. (Right) Axial T1WI MR depicts propagation of respiratory motion  through the abdomen and spine, as well as phase wrap of the abdomen behind the back .

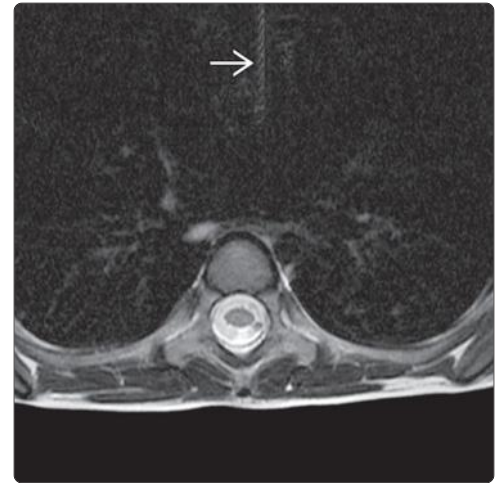



(Left) Sagittal T2WI MR shows marked signal loss and image degradation in the upper thoracic spine, reflecting attempted MR imaging with the incorrect spine coil elements turned on. There is also a prominent zipper artifact  running in the craniocaudal direction. (Right) Sagittal T1WI MR reveals marked distortion of the inferior frontal lobes and facial soft tissues reflecting severe metallic dental brace artifact.

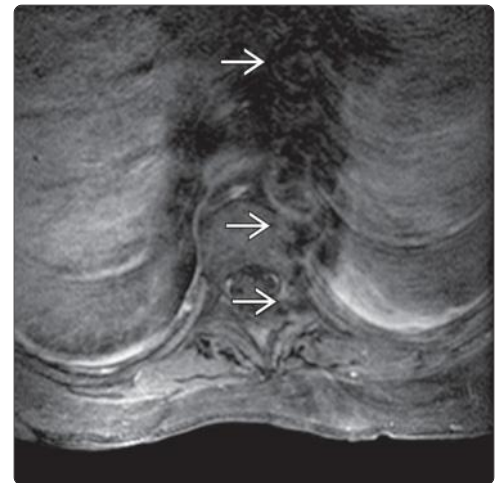
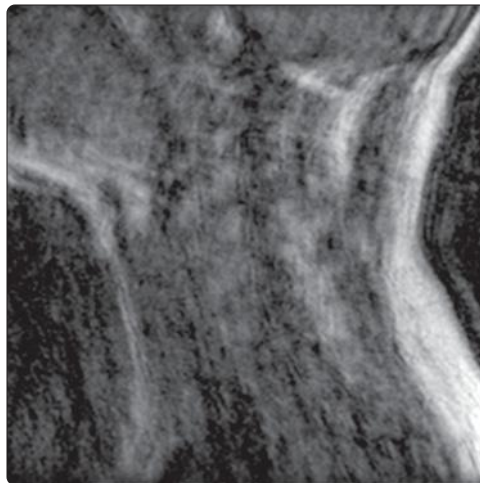
**(Left)** Sagittal T1WI MR (suprasellar craniopharyngioma, postoperative) performed for spinal surveillance with known CSF craniopharyngioma dissemination shows a metastatic lesion  anterior to the pons. **(Right)** Sagittal T1WI C+ FS MR (suprasellar craniopharyngioma, known CSF metastases) demonstrates a prominent band of susceptibility artifact  2° to inhomogeneous fat saturation, unfortunately nearly completely obscuring known CSF metastasis .



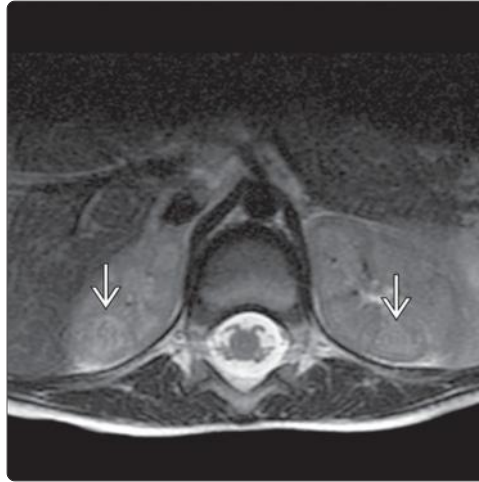
**(Left)** Sagittal T1WI MR shows severe radiofrequency interference artifact creating horizontal stripes across the image producing mild image degradation. Note also the incomplete zipper artifact  at the inferior margin of the image center. **(Right)** Axial T2WI MR of the thoracic spine demonstrates a prominent zipper artifact  in the upper center of the image. Like most zipper artifacts, this does not seriously compromise the diagnostic quality of the exam.






**(Left)** Sagittal T1WI MR in an uncooperative, delirious patient shows severe motion artifact that markedly degrades the image quality and renders it nondiagnostic. It is important not to try to use these images in a diagnostic attempt, because artifact may either simulate or obscure a lesion. **(Right)** Axial T1WI C+ FS MR shows severe motion artifact running in the AP direction reflecting respiratory movement of the abdominal wall. There is also periodic phase ghosting of the aorta .

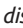



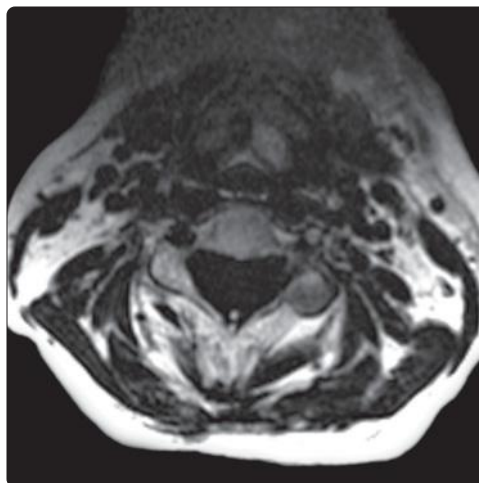
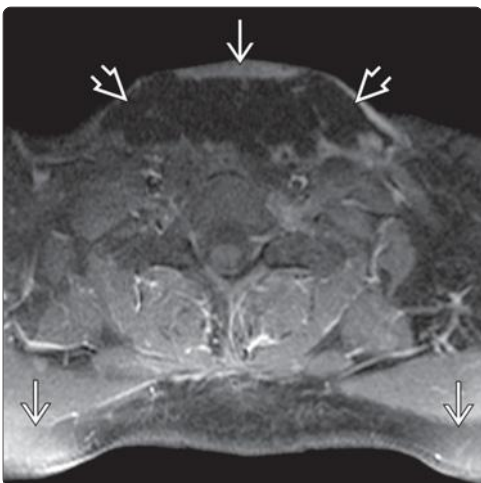



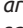


(Left) Axial T2WI MR depicts periodic phase encoding artifact from the thecal sac simulating lesions in the liver  and spleen . The spacing between the thecal sac and the artifactual ghosts is precisely the same distance, a characteristic finding with periodic phase ghosting artifact. Recognizing this assists in making the diagnosis of artifact. (Right) Axial T2WI MR shows periodic phase ghosting from the thecal sac and spinal cord simulating bilateral renal lesions .



(Left) Sagittal T1WI MR demonstrates gradient warping artifact of the lower thoracic spine. This artifact is characterized by image distortion  at the edges of large FOV studies (esp. > 30 cm) caused by gradient distortion. (Right) Sagittal T2WI MR depicts unacceptable phase ghosting artifact  that mimics cervical syringohydromyelia in this case arising from failure to place an anterior saturation band in front of the cervical spine.



(Left) Axial T1WI C+ FS MR shows inhomogeneous fat suppression using chemical fat-saturation technique, with bright areas of fat-suppression failure , as well as dark areas of inappropriate water saturation . (Right) Axial T1WI C+ FS MR shows complete failure of chemical fat-saturation technique, compounded by unwanted inappropriate water saturation that nullifies all water signal. This artifact is commonly encountered when imaging complex shapes such as the cervicothoracic junction.

## KEY FACTS

### TERMINOLOGY

- Normal anatomical variations that simulate pathological conditions

### IMAGING

- Multiplanar MR best for soft tissue evaluation
- Radiography, bone CT most useful for bone anatomy

### TOP DIFFERENTIAL DIAGNOSES

- Traumatic or degenerative vertebral subluxation
- Transverse process fracture
- Vertebral segmentation and formation anomalies
- Vertebral hemangioma
- Intervertebral disc herniation
- Nerve sheath tumor
- Posterior spinal dysraphism
- Caudal regression spectrum

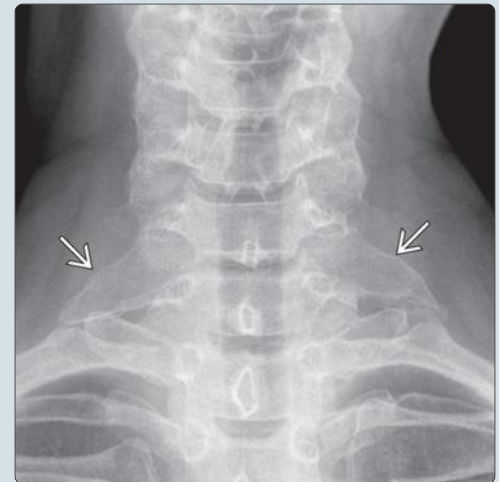
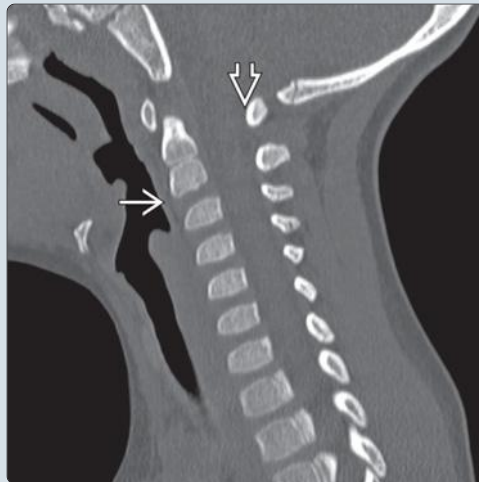
### CLINICAL ISSUES

- Discovered incidentally when patient is imaged for other indications
  - Patient asymptomatic, or presenting symptoms do not match location of finding
- Normal life expectancy, no incremental morbidity
- May lead to unnecessary diagnostic tests or treatment if not recognized as normal variant

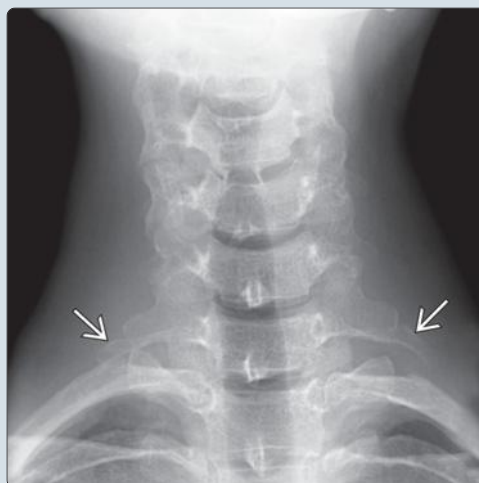
### DIAGNOSTIC CHECKLIST

- Many normal variants are common and readily recognized by experienced observers
- Some are uncommon and may not be recognized as normal variant, require high index of suspicion to correctly diagnose
- Consider normal variant within differential diagnostic considerations when unexpected finding is detected

**(Left)** Sagittal bone CT in a young pediatric patient demonstrates slight apparent subluxation of C2 on C3. All other spinal lines are normal, particularly the posterior spinolaminar line from C1 to C3, confirming pseudosubluxation. **(Right)** Anteroposterior cervical radiograph shows unusual elongation of the C7 transverse processes. In some patients, draping of the lower brachial plexus trunk over the C7 transverse process may produce a clinical brachial plexopathy.



**(Left)** Anteroposterior cervical radiograph demonstrates small bilateral rudimentary C7 cervical ribs. Downward angulation of the adjacent transverse processes distinguishes these from hypoplastic T1 thoracic ribs. **(Right)** Sagittal T1WI MR along the plane of the medial aspect of the L5 pedicle shows a vertically oriented root spanning the L5 disc level due to a conjoined nerve root. This vertical orientation of the exiting inferior root is typical, along with the more horizontal course of the superior root.



## TERMINOLOGY

### Definitions

- Normal anatomical variations that simulate pathological conditions

## IMAGING

### Cervical Vertebral Pseudosubluxation

- Classically most conspicuous at C2/3 level, with apparent anterior subluxation of C2 on C3 with head in flexed position
- Observed in younger pediatric patients with incomplete ossification of upper cervical spine
  - Prevalence in older patients controversial, may represent true ligamentous injury
- Absence of spinolaminar line disruption and patient age keys to correct recognition

### Incomplete C1 Ring

- C1 ring is incompletely ossified
- In absence of neurological abnormalities or documented instability, asymptomatic normal variant detected during imaging for other reasons

### Cervical Ribs

- Small rudimentary ribs at C7
  - Elongation of C7 transverse processes is close variant with similar clinical findings
- Usually asymptomatic but may produce brachial plexopathy or thoracic outlet symptoms
- Orientation of transverse processes key to distinguishing cervical from thoracic ribs
  - Cervical transverse processes point caudal, while thoracic transverse processes point rostral

### Transitional Vertebral Anatomy

- Variant osseous anatomy at thoracolumbar or lumbosacral transitions
- Common variants include S1 "lumbarization," L5 "sacralization," rudimentary L1 ribs, hypoplastic T12 ribs
- Confound correct counting of vertebral levels
  - Usually not clinically significant issue if counting method well described in imaging report
- May predispose to accelerated degenerative changes at mobile segments above or below variant levels

### Focal Fatty Marrow

- Focal fat conglomeration within vertebral marrow
- Follows fat signal and density on all sequences
  - Fat-saturation MR sequences helpful to confirm diagnosis
- Primary clinical impact is mimicry of vertebral hemangioma

### Ectopic Kidney

- Pelvic kidney lower than orthotopic location, more midline than expected
- May mimic prevertebral neoplasm
- Correct identification of corticomedullary reniform architecture critical to avoid unnecessary biopsy or resection

### Conjoined Nerve Root

- 2 adjacent spinal nerve roots exit through a common aberrant nerve root sleeve
- Nerves subsequently either exit individually through correct-numbered neural foramina or both through a single foramen
- Mimics nerve sheath tumor or intervertebral disc herniation on imaging

### Incomplete Posterior Lumbar Elements

- Incomplete fusion of L5 or S1 posterior elements
  - Term "spina bifida occulta" outdated and use is discouraged
- Commonly observed in asymptomatic population
- Should be considered normal variant in absence of cutaneous abnormalities or referable neurological abnormalities

### High Thecal Sac Termination

- Normal thecal sac termination usually inferior S2 level
  - Range from lower 1/3 of L3 → upper 1/3 of S5
  - < 5% terminate above S1 level
- Normal neurological examination expected with incidental anatomic variant
- Spinal cord anomalies or sacral dysplasia prompts consideration of caudal regression spectrum

### Imaging Recommendations

- Best imaging tool
  - Multiplanar MR best for soft tissue evaluation
  - Plain radiographs, bone CT most useful for working out bone anatomy

## DIFFERENTIAL DIAGNOSIS

### Traumatic or Degenerative Vertebral Subluxation

- Mimics cervical pseudosubluxation
- True listhesis secondary to trauma or degenerative changes
- Characteristically demonstrates spinolaminar line disruption, in contradistinction to cervical pseudosubluxation
- Concurrent fractures or degenerative osseous changes common
- Patients generally much older than pseudosubluxation age range

### Transverse Process Fracture

- Mimics cervical rib or hypoplastic thoracic or lumbar rib
- Sharp, noncorticated edge at fracture site
- ± paraspinal hematoma, other injuries

### Vertebral Segmentation and Formation Anomalies

- True failure of normal vertebral formation or segmentation
  - Butterfly and hemivertebra, block vertebra, posterior element fusion
- Mimics variant transitional thoracolumbar or lumbosacral anatomy
- Consider syndromal associations, concurrent visceral anomalies

### Vertebral Hemangioma

- Mimics focal fatty vertebral marrow

- Most are asymptomatic and incidentally discovered on imaging for other indications
  - Small percentage have atypical vascular (nonfatty) stroma, may extend beyond vertebral body, pathological fracture
  - Primary clinical importance has resemblance to primary or metastatic vertebral malignancy
- Round shape, coarsened vertebral trabeculae help confirm benign hemangioma diagnosis

### Intervertebral Disc Herniation

- Mimics conjoined nerve root, nerve sheath tumor
- Protean imaging appearances
  - Disc fragment does not homogeneously enhance, helping to distinguish from a nerve sheath tumor or normal dorsal root ganglion
  - May resemble conjoined nerve root; look for increased number of nerves in root sleeve, aberrant nerve sheath origin

### Nerve Sheath Tumor

- Mimics conjoined nerve root, intervertebral disc herniation
- Neurofibroma, schwannoma most common spinal nerve neoplasms
- Enhancement pattern helps distinguish from normal or conjoined nerve root, herniated intervertebral disc

### Posterior Spinal Dysraphism

- Mimics incidental variant incomplete posterior element fusion
- May be open or closed (skin-covered)
- Frequently coexists with low-lying spinal cord and filum anomalies ± lipoma

### Caudal Regression Spectrum

- Mimics isolated incidental high thecal sac termination
- < 5 sacral segments + coccyx by definition
- Spinal cord either wedge-shaped, high termination (type 1) or elongated and low-lying (type 2)
- Association with pelvic visceral anomalies, other congenital spinal malformations

## PATHOLOGY

### General Features

- Etiology
  - Normal variant

### Gross Pathologic & Surgical Features

- Concordant with imaging features

### Microscopic Features

- Characteristic of tissue composition

## CLINICAL ISSUES

### Presentation

- Most common signs/symptoms
  - Discovered incidentally when patient is imaged for other indications
  - Patient asymptomatic or presenting symptoms that prompt imaging does not match location of findings

### Demographics

- Age
  - Detection possible throughout entire life span
- Epidemiology
  - Variable

### Natural History & Prognosis

- Normal variant; does not alter normal life expectancy or produce morbidity
- May lead to unnecessary diagnostic tests or treatment if not recognized as normal variant

### Treatment

- None indicated

## DIAGNOSTIC CHECKLIST

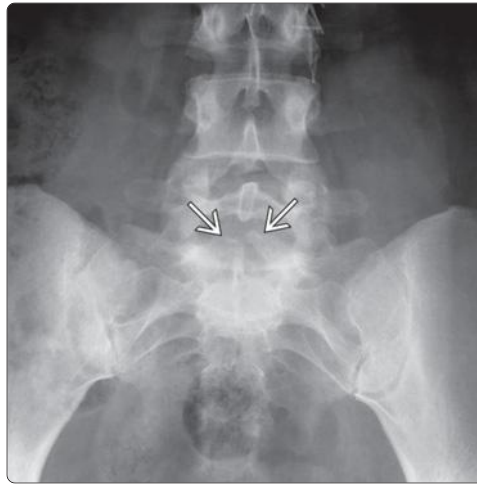
### Consider

- Many normal variants are common
  - Readily recognized by experienced observers
- Some are uncommon enough that may not be recognized as normal variant
  - Require high index of suspicion to correctly diagnose
  - Consider normal variant within differential diagnostic considerations when unexpected finding is detected

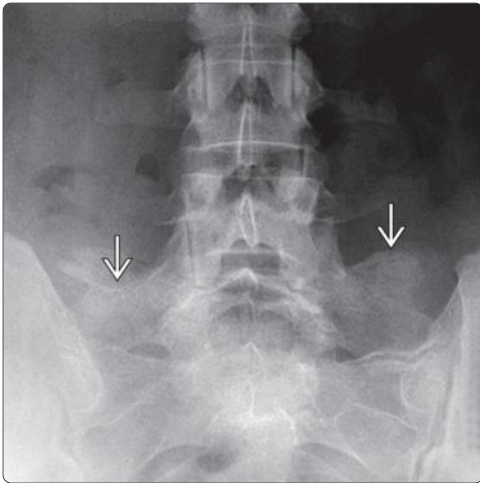
## SELECTED REFERENCES

1. Thawait GK et al: Spine segmentation and enumeration and normal variants. *Radiol Clin North Am.* 50(4):587-98, 2012
2. Gaca AM et al: Evaluation of wedging of lower thoracic and upper lumbar vertebral bodies in the pediatric population. *AJR Am J Roentgenol.* 194(2):516-20, 2010
3. Hanson EH et al: Sagittal whole-spine magnetic resonance imaging in 750 consecutive outpatients: accurate determination of the number of lumbar vertebral bodies. *J Neurosurg Spine.* 12(1):47-55, 2010
4. Lotan R et al: Clinical features of conjoined lumbosacral nerve roots versus lumbar intervertebral disc herniations. *Eur Spine J.* 19(7):1094-8, 2010
5. De Martino RR et al: Thoracic outlet syndrome associated with a large cervical rib. *Vasc Endovascular Surg.* 43(4):393-4, 2009
6. Kanchan T et al: Lumbosacral transitional vertebra: clinical and forensic implications. *Singapore Med J.* 50(2):e85-7, 2009
7. White PW et al: Cervical rib causing arterial thoracic outlet syndrome. *J Am Coll Surg.* 209(1):148-9, 2009
8. Song SJ et al: Imaging features suggestive of a conjoined nerve root on routine axial MRI. *Skeletal Radiol.* 37(2):133-8, 2008
9. Serhan HA et al: Biomechanics of the posterior lumbar articulating elements. *Neurosurg Focus.* 22(1):E1, 2007
10. Soleiman J et al: Magnetic resonance imaging study of the level of termination of the conus medullaris and the thecal sac: influence of age and gender. *Spine (Phila Pa 1976).* 30(16):1875-80, 2005
11. Lustrin ES et al: Pediatric cervical spine: normal anatomy, variants, and trauma. *Radiographics.* 23(3):539-60, 2003
12. Shaw M et al: Pseudosubluxation of C2 on C3 in polytraumatized children—prevalence and significance. *Clin Radiol.* 54(6):377-80, 1999
13. Castellvi AE et al: Lumbosacral transitional vertebrae and their relationship with lumbar extradural defects. *Spine (Phila Pa 1976).* 9(5):493-5, 1984

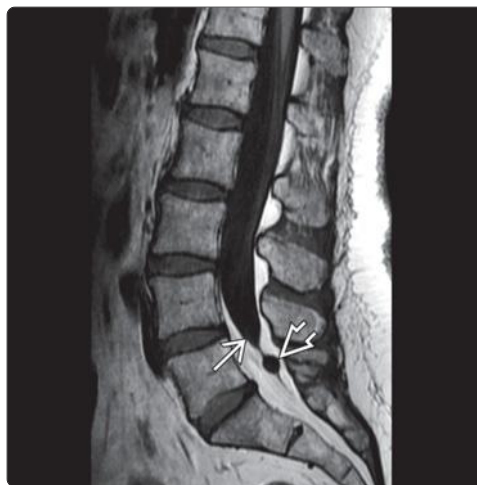
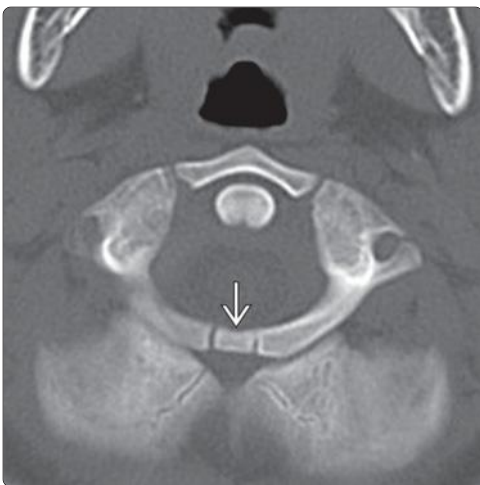




(Left) Sagittal T1WI MR of the thoracic spine demonstrates focal, well-circumscribed hyperintense signal intensity within a mid-thoracic vertebral body. There is no disruption of the posterior vertebra. The differential is focal fatty marrows vs. a small hemangioma. Both are of no clinical consequence. (Right) Anteroposterior radiograph of the lumbar spine obtained for low back pain reveals incidental incomplete posterior fusion of the S1 lamina in the midline.



(Left) Anteroposterior radiograph shows incorporation of the L5 transverse processes into the sacral ala bilaterally ("sacralization of L5"). (Right) Axial T1WI MR of the sacral spine depicts 2 ovoid masses within the right S1 foramen representing conjoined nerve roots.



(Left) Axial bone CT shows a variant accessory ossification center in the midline of the posterior C1 arch. The anterior C1 ring shows conventional anatomy with a single ossification center. This uncommon variant is asymptomatic and stable. (Right) Sagittal T1WI MR (normal neurological examination) demonstrates incidentally detected high termination of the thecal sac at the mid-L5 level with a small perineural cyst. The conus terminates at the normal L1 level, and the filum terminale is not thickened.



# Craniovertebral Junction Variants

## KEY FACTS

### TERMINOLOGY

- Anomalous or variant craniovertebral junction anatomy

### IMAGING

- Flattening or malformation of clivus/occipital condyles, anterior C1 ring, or dens
- Variable instability during dynamic flexion, extension
- ± enhancing granulation tissue mass ("pannus")
  - Reducible abnormalities have largest pannus

### TOP DIFFERENTIAL DIAGNOSES

- Developmental CVJ anomalies
  - Achondroplasia, Down syndrome
- Inflammatory and degenerative arthritides
- Acquired basilar impression
- Trauma

### PATHOLOGY

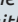
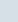

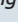
- Congenital insult to developing CVJ neural and osseous tissue between 4th and 7th intrauterine weeks
- Solid ankylosis or fibrous union in many irreducible anomalies
- Granulation tissue proliferation around motion areas in unstable or reducible anomalies

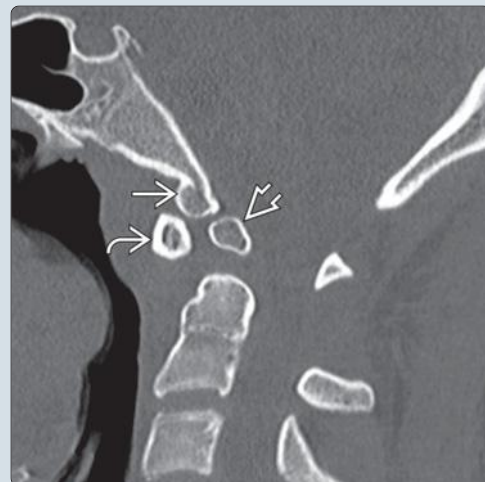
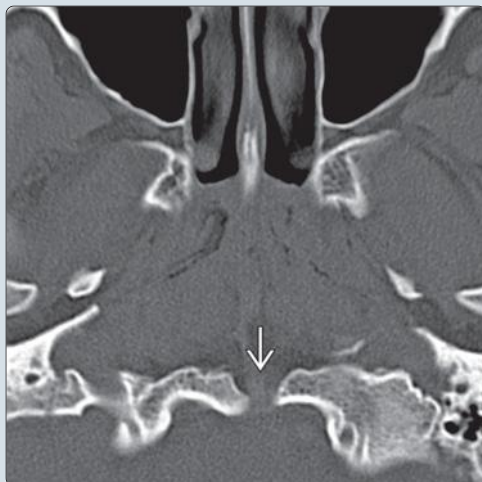
### CLINICAL ISSUES

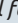
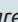
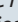
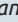
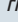
- Occipital headache or suboccipital neck pain exacerbated by flexion/extension
- Symptomatic presentation following mild trauma common

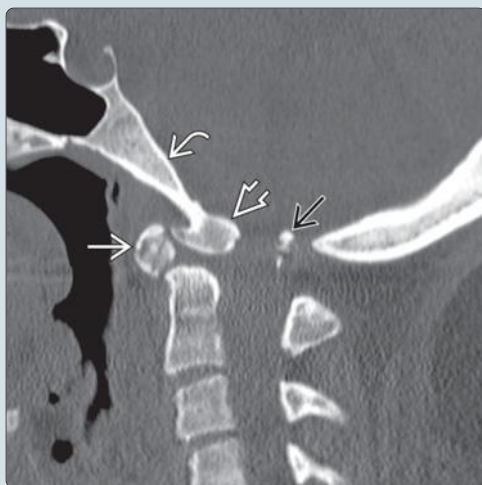
### DIAGNOSTIC CHECKLIST

- Dynamic flex-extend imaging determines stability, reducibility of abnormality

**(Left)** Axial bone CT (platybasia) reveals an aberrant, flattened clivus with unusual coronal orientation. Also demonstrated is a prominent midline bone cleft defect . **(Right)** Sagittal bone CT demonstrates coexisting condylus tertius and os odontoideum in a patient with atlantoaxial instability. Note the osseous protrusion from the clivus tip  representing the condylus tertius. The os  is dystopic, and the anterior C1 ring  is enlarged.



**(Left)** Sagittal bone CT (os avis) reveals abnormal fusion of the os  to the clivus . Remodeling changes are also noted in the anterior C1 ring  and os. The posterior C1 ring  is hypoplastic and resides within the spinal canal, just below the foramen magnum. **(Right)** Sagittal FLAIR (os avis, same patient) reveals abnormal T2 signal within the cervical spinal cord at the C1 level, reflecting injury related to atlantoaxial instability and mild C1 ring  hypoplasia.



## TERMINOLOGY

### Abbreviations

- Craniovertebral junction (CVJ), craniocerebral junction (CCJ)

### Synonyms

- CVJ anomalies, CCJ variants or anomalies

### Definitions

- Anatomical variations of skull base-upper cervical spine articulation

## IMAGING

### General Features

- Best diagnostic clue
  - Flattening or malformation of clivus/occipital condyles, anterior C1 ring, or odontoid process

### Radiographic Findings

- Radiography
  - Platybasia, basilar invagination, C1 ring assimilation, asymmetrical C1/2 articulation, backward tilt, hypoplasia/aplasia, os odontoideum of odontoid process, C2/3 fusion (Klippel-Feil)

### Fluoroscopic Findings

- Variable instability of C0/1, C1/2 articulations with dynamic flexion and extension

### CT Findings

- CECT
  - ± enhancing granulation tissue mass ("pannus")
    - Patients with reducible abnormalities usually have largest pannus
- Bone CT
  - Findings similar to plain radiographs; sagittal and coronal reformats minimize effect of overlapping structures

### MR Findings

- T1WI
  - Osseous anomalies ± soft tissue granulation tissue, cord compression, hindbrain anomalies
- T2WI
  - Similar to T1WI; best for evaluating spinal cord
- T1WI C+
  - ± enhancing "pannus"

### Imaging Recommendations

- Protocol advice
  - Dynamic flex-extend plain films to demonstrate biomechanics, uncover instability
  - Multiplanar T1WI, T2WI to evaluate cord, soft tissues; flex-extend MR optimally delineates effect of position on neural compression
  - Bone CT with multiplanar reformats to evaluate osseous structures for surgical planning

## DIFFERENTIAL DIAGNOSIS

### Developmental CVJ Anomalies

- CVJ stenosis or atlantoaxial instability 2° to
  - Achondroplasia

- Mucopolysaccharidosis
- Down syndrome
- Inborn errors of metabolism

### Inflammatory and Degenerative Arthritides

- ± CVJ fusion, anterior displacement of C1 ring from dens, basilar invagination → possible cord compression 2° to canal stenosis
  - Rheumatoid arthritides
  - Reactive arthritides
  - Psoriatic arthritides
  - Ankylosing spondylitis
  - Degenerative arthritis (osteoarthritis)
- Clinical manifestations include myelopathy, pain, extremity deformity
  - Elicit characteristic clinical, historical, and laboratory abnormalities to confirm diagnosis

### Acquired Basilar Impression

- Upward displacement of occipital condyles above plane of foramen magnum, radiological protrusion of dens tip above Chamberlain line
- 2° to bone softening
  - Paget disease
  - Osteogenesis imperfecta
  - Rickets
  - Rheumatoid arthritis
  - Hyperparathyroidism

### Trauma

- CVJ injuries relatively uncommon but high morbidity/mortality
- Fracture &/or ligamentous injury
- Sharp, noncorticated margins argue against congenital anomaly

## PATHOLOGY

### General Features

- Etiology
  - Congenital insult to developing CVJ neural and osseous tissue between 4th and 7th intrauterine weeks → hypoplasia, segmentation/fusion anomalies, CVJ ankylosis
- Associated abnormalities
  - Dwarfism, jaw anomalies, cleft palate, congenital ear deformities, short neck, Sprengel deformity, funnel chest, pes cavus, and syndactyly
- Congenital CVJ abnormalities are relatively uncommon
  - Severity ranges from benign, asymptomatic to potentially fatal instability → cord/brainstem compression
- Type and severity of anomaly determined by anatomy relative to 1 or more standard "lines of reference"
  - Chamberlain line: Line drawn from opisthion to dorsal margin of hard palate
  - McGregor line: Line drawn from upper posterior hard palate to most caudad point of occiput

### Staging, Grading, & Classification

- Occipital sclerotome malformations

- Most occiput anomalies associated with ↓ skull base height ± basilar invagination (odontoid tip > 4.5 mm above McGregor line)
  - Condylus tertius, condylar hypoplasia, basiocciput hypoplasia, atlantooccipital assimilation, bifid clivus
  - Platybasia = congenital flattening of craniocervical angle > 135°
  - Associated with hindbrain herniation, syringomyelia (≤ 30%)
- C1 ring anomalies
  - C1 assimilation ("occipitalized C1"): Segmentation failure → fibrous or osseous union between 1st spinal sclerotome and 4th occipital sclerotome
    - ± occipitocervical synostosis; most C1 ring assimilations asymptomatic, more likely to be symptomatic if retroodontoid AP canal diameter < 19 mm
  - C1 malformation: Aplasia, hypoplasia, cleft C1 arch, "split atlas" (anterior and posterior arch rachischisis)
  - Association with Klippel-Feil, basilar invagination, Chiari 1 malformation
- C2 anomalies: C1/2 segmentation failure, dens dysplasia
  - Majority confined to odontoid process; partial (hypoplasia) → complete absence (aplasia), ossiculum terminale persists, os odontoideum
    - Ossiculum terminale persists: Ossification failure of terminal ossicle → incidental "notch" in dens tip
    - Os odontoideum: Well-defined ossicle at dens tip + anterior C1 arch enlargement
  - Odontoid anomalies in association with ligamentous laxity → atlantoaxial instability
    - Incompetence of cruciate ligament → C1/2 instability, possible neurologic deficit, or death
    - Most common in Down syndrome, Morquio syndrome, Klippel-Feil syndrome, & skeletal dysplasias

## Gross Pathologic & Surgical Features

- Solid ankylosis or fibrous union in many irreducible anomalies
- Granulation tissue proliferation around motion areas in unstable or reducible anomalies

## Microscopic Features

- Variable components of histologically normal bone, fibrous tissue, & granulation tissue

## CLINICAL ISSUES

### Presentation

- Most common signs/symptoms
  - Suboccipital neck pain (85%); may clinically mimic "basilar migraine"
  - Posterior occipital headache exacerbated by flexion/extension
- Other signs/symptoms
  - Myelopathy, brainstem/cranial nerve deficits, weakness, lower extremity ataxia
  - Vascular symptoms (15-20%); TIA, vertigo, visual symptoms with rotation or head manipulation
- Clinical profile
  - Usually normal clinical appearance; obvious clinical dysmorphism implies syndromal association

- Symptomatic presentation following mild trauma common

## Demographics

- Age
  - Infancy → late adulthood depending on severity
- Gender
  - M = F
- Epidemiology
  - Relatively uncommon: 0.14-0.25% pediatric population

## Natural History & Prognosis

- Usually gradual onset of neurological symptoms with localizing signs; some patients asymptomatic throughout life
- Occasionally, neurological presentation is fulminant → quadriplegia, sudden death
- Undetected anomalies at risk for injury during minor trauma, anesthesia
- Early diagnosis permits treatment before symptoms or permanent neurological sequelae

## Treatment

- Conservative approach initially unless unstable or neural deficits present
  - Traction, cervical orthosis, activity restriction
- Symptomatic, refractory to conservative management
  - Skeletal traction to distinguish reducible from irreducible abnormalities, relieve symptoms preoperatively
  - Correction of underlying biomechanical abnormality with decompression ± fusion

## DIAGNOSTIC CHECKLIST

### Consider

- Look for combinations of anomalies based on known association patterns
- Impact of diagnosis must be customized to individual patient to develop best treatment approach

### Image Interpretation Pearls

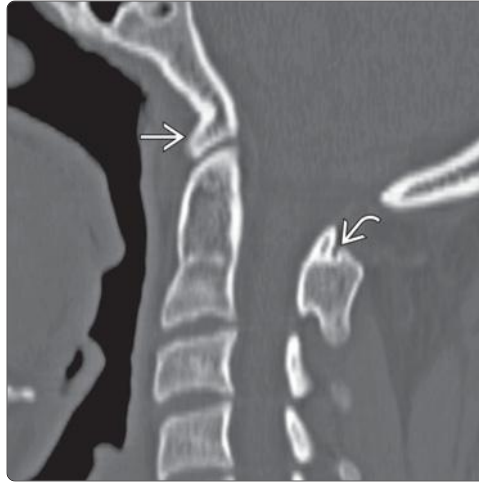
- Dynamic flex-extend imaging determines stability, reducibility of abnormality
- CT with reformats valuable for evaluating osseous abnormalities

## SELECTED REFERENCES

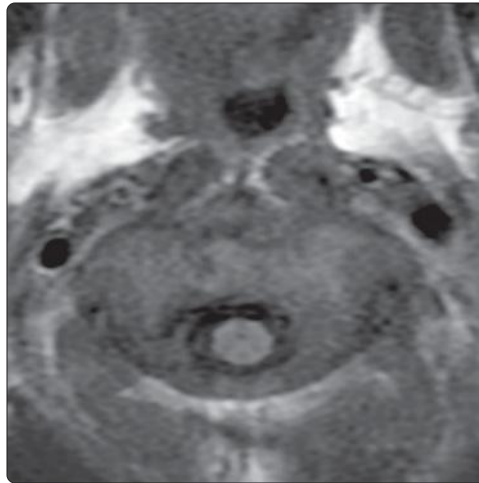
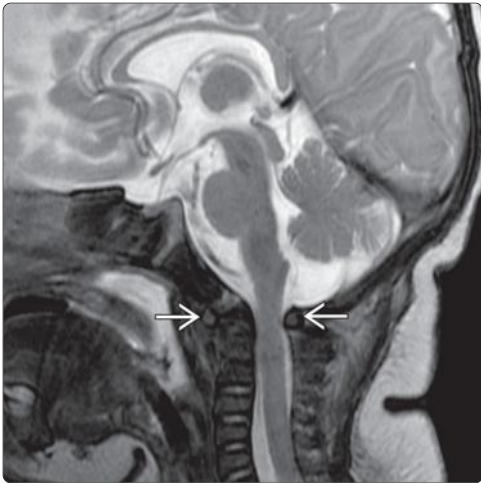
1. Menezes AH: Nosographic identification and management of pediatric craniovertebral junction anomalies: evolution of concepts and modalities of treatment. *Adv Tech Stand Neurosurg.* 40:3-18, 2014
2. Natung T et al: Symmetrical chorioretinal colobomata with craniovertebral junction anomalies in CHARGE syndrome - a case report with review of literature. *J Clin Imaging Sci.* 4:5, 2014
3. Shetty SR et al: Neurenteric cyst at the craniovertebral junction: A report of two cases. *Asian J Neurosurg.* 8(4):188-91, 2013
4. Menezes AH: Craniocervical fusions in children. *J Neurosurg Pediatr.* 9(6):573-85, 2012
5. Menezes AH: Craniocervical developmental anatomy and its implications. *Childs Nerv Syst.* 24(10):1109-22, 2008
6. Smoker WR et al: Imaging the craniocervical junction. *Childs Nerv Syst.* 24(10):1123-45, 2008



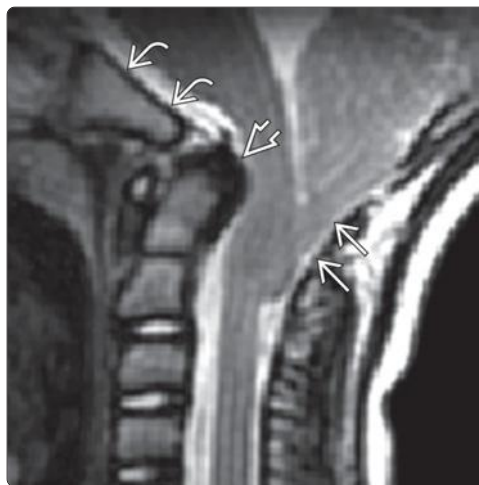
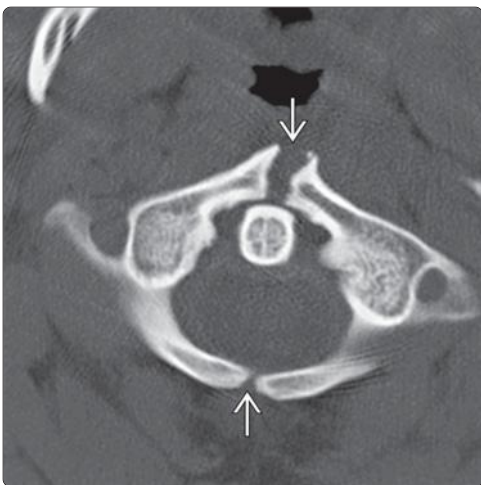
# Craniovertebral Junction Variants



(Left) Sagittal bone CT shows assimilation of anterior C1 ring with basion and partial assimilation of posterior C1 arch with opisthion. There is widened atlantodental interval and mild basilar invagination. (Right) Sagittal bone CT demonstrates congenital assimilation of anterior C1 ring with clivus as well as fusion of the posterior C1 ring to the C2 spinous process. This CVJ anatomical variation would be expected to produce reduced CVJ dynamic motion.



(Left) Sagittal T2WI MR (VACTERL) shows moderately severe central canal stenosis at C1 secondary to C1 ring hypoplasia. There is mild T2 hyperintense signal in the cord at that level indicating myelomalacia. Also incidentally demonstrated is a rudimentary intervertebral disc space at C2-C3, reflecting congenital segmentation failure. (Right) Axial T1WI (VACTERL) MR confirms moderately severe central canal stenosis at C1 secondary to C1 ring hypoplasia.



(Left) Axial bone CT depicts congenital fusion failure of the C1 ring, with both anterior and posterior ring clefts. Despite its bizarre appearance, this constellation of findings does not necessarily predispose to cervical instability. (Right) Sagittal T2WI MR reveals flattening of the clivus angle and aberrant odontoid retroflexion with adjacent hypointense pannus. In addition, MR imaging discloses a previously unsuspected Chiari 1 malformation with cerebellar tonsillar ectopia.



# Ponticulus Posticus

## KEY FACTS

### TERMINOLOGY

- Latin: "Little posterior bridge"
- Synonyms: Arcuate foramen, sagittal foramen, canalis vertebralis, retroarticular canal, retroarticular/retrocondylar vertebral artery ring, upper retroarticular foramen, and atlantal posterior foramen

### IMAGING

- Osseous roof along superior C1 arch covers C1 vertebral artery foramen
  - Vertebral artery passes through osseous tunnel
- May be partial or complete
- Unilateral or bilateral

### TOP DIFFERENTIAL DIAGNOSES

- Broad C1 posterior arch

### PATHOLOGY

- Postulated to arise from ossification of lateral segment of posterior atlantooccipital ligament or joint capsule

- Morphologically normal bone

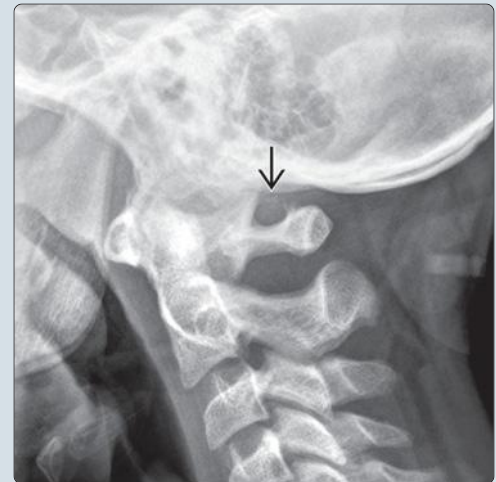
### CLINICAL ISSUES

- Most common: Asymptomatic
- Other symptoms
  - Vertebrobasilar ischemia or infarction
  - Vertigo
  - Headache
  - Neck pain

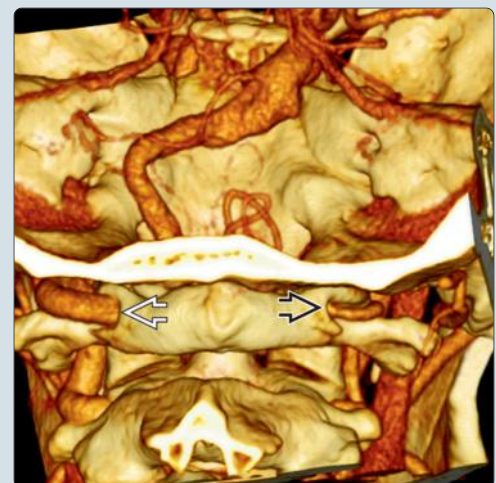
### DIAGNOSTIC CHECKLIST

- Vertebral arteries predisposed to surgical injury during lateral mass screw placement
- Multiplanar bone CT with 3D reformats best demonstrates ponticulus posticus

**(Left)** Lateral radiograph of the upper cervical spine demonstrates a partial osseous roof over the C1 vertebral artery foramen, characteristic of ponticulus posticus (incomplete variant). **(Right)** Lateral radiography of the upper cervical spine reveals a complete osseous roof over the C1 vertebral artery foramen, typical of classic ponticulus posticus (complete variant).



**(Left)** Sagittal CTA depicts a complete C1 arch, with a robust osseous covering (complete ponticulus posticus) over the vertebral artery along the superior aspect of the C1 arch. **(Right)** Anteroposterior view of a CTA 3D reformat shows a dominant left vertebral artery and smaller (nondominant) right vertebral artery. Both are covered by a complete osseous bridge along the superior aspect of the C1 arch.



## TERMINOLOGY

### Synonyms

- Arcuate foramen, sagittal foramen, canalis vertebralis, retroarticular canal, retroarticular/retrocondylar vertebral artery ring, upper retroarticular foramen, and atlantal posterior foramen

### Definitions

- Osseous arch connecting retroglenoid tubercle with posterior C1 arch
- Latin: "Little posterior bridge"

## IMAGING

### General Features

- Best diagnostic clue
  - Osseous "bridge" along superior C1 arch covers vertebral artery
- Location
  - C1 arch vertebral foramen
  - Unilateral or bilateral
- Morphology
  - May be partial or complete

### Radiographic Findings

- Radiography
  - Partial or complete osseous roof over C1 vertebral artery foramen

### CT Findings

- Bone CT
  - Complete or incomplete osseous "bridge" covers C1 vertebral foramen
- CTA
  - Vertebral artery passes through osseous tunnel formed by ponticulus posticus

### MR Findings

- Partial or complete osseous roof over C1 vertebral artery foramen
- MRA
  - Contains ipsilateral vertebral artery

### Imaging Recommendations

- Best imaging tool
  - Multiplanar bone CT with 3D reformats

## DIFFERENTIAL DIAGNOSIS

### Broad C1 Posterior Arch

- Mistaking ponticulus posticus for broad posterior C1 arch → vertebral artery injury during C1 lateral mass screw placement

## PATHOLOGY

### General Features

- Etiology
  - Postulated to arise from ossification of lateral segment of posterior atlantooccipital ligament or joint capsule
- Associated abnormalities
  - None

## Staging, Grading, & Classification

- Full: Complete osseous ring
- Incomplete: Portions of osseous ring absent
- Calcified: Linear or amorphous calcification

## Gross Pathologic & Surgical Features

- Morphologically normal bone
- May mimic posterior C1 arch

## CLINICAL ISSUES

### Presentation

- Most common signs/symptoms
  - Asymptomatic
- Other signs/symptoms
  - Vertebrobasilar ischemia or infarction
  - Vertigo
  - Headache
  - Neck pain
  - Shoulder/arm pain

### Demographics

- Age
  - No association
- Gender
  - F > M
- Epidemiology
  - 3-38%

## DIAGNOSTIC CHECKLIST

### Consider

- Vertebral arteries predisposed to surgical injury during lateral mass screw placement
- Multiplanar bone CT with 3D reformats best demonstrates ponticulus posticus

## SELECTED REFERENCES

1. O' Donnell CM et al: Vertebral artery anomalies at the craniovertebral junction in the US population. *Spine (Phila Pa 1976)*. 39(18):E1053-7, 2014
2. Lee SH et al: Posterior C1-2 fusion using a polyaxial screw/rod system for os odontoideum with bilateral persistence of the first intersegmental artery. *J Neurosurg Spine*. 14(1):10-3, 2011
3. Mellado JM et al: MDCT of variations and anomalies of the neural arch and its processes: part 2--articular processes, transverse processes, and high cervical spine. *AJR Am J Roentgenol*. 197(1):W114-21, 2011
4. Greiner HM et al: Rotational vertebral artery occlusion in a child with multiple strokes: a case-based update. *Childs Nerv Syst*. 26(12):1669-74, 2010
5. Koutsouraki E et al: Kimmerle's anomaly as a possible causative factor of chronic tension-type headaches and neurosensory hearing loss: case report and literature review. *Int J Neurosci*. 120(3):236-9, 2010
6. Sharma V et al: Prevalence of ponticulus posticus in Indian orthodontic patients. *Dentomaxillofac Radiol*. 39(5):277-83, 2010
7. Kim KH et al: Prevalence and morphologic features of ponticulus posticus in Koreans: analysis of 312 radiographs and 225 three-dimensional CT scans. *Asian Spine J*. 1(1):27-31, 2007
8. Cakmak O et al: Arcuate foramen and its clinical significance. *Saudi Med J*. 26(9):1409-13, 2005
9. Young JP et al: The ponticulus posticus: implications for screw insertion into the first cervical lateral mass. *J Bone Joint Surg Am*. 87(11):2495-8, 2005
10. Cushing KE et al: Tethering of the vertebral artery in the congenital arcuate foramen of the atlas vertebra: a possible cause of vertebral artery dissection in children. *Dev Med Child Neurol*. 43(7):491-6, 2001
11. Wight S et al: Incidence of ponticulus posterior of the atlas in migraine and cervicogenic headache. *J Manipulative Physiol Ther*. 22(1):15-20, 1999

## KEY FACTS

### TERMINOLOGY

- Synonym: Ossiculum terminale persistens
- Persistence of unfused odontoid tip ossification center into adulthood

### IMAGING

- Separate ossicle with intact cortical margin positioned above normal-sized odontoid process in adolescent or adult
  - May be dystopic or orthotopic
- Soft tissue pannus suggests atlantoaxial instability
- Myelomalacia, brainstem compression in rare cases

### TOP DIFFERENTIAL DIAGNOSES

- Os odontoideum
- Type I or II odontoid fracture
- Normal unfused odontoid tip synchondrosis
- Degenerative remodeling of odontoid process

### PATHOLOGY

- Terminal ossicle normally appears by 3 years of age, fuses with odontoid body by 12 years of age
- Terminal ossicle located above transverse ligament
  - Atlantoaxial instability less common than with os odontoideum
  - Unstable ossiculum terminale usually dystopic

### CLINICAL ISSUES

- Usually asymptomatic
- Uncommonly, neck pain or myelopathy related to CVJ instability

### DIAGNOSTIC CHECKLIST

- Consider ossiculum terminale in patients > 12 years with persistent terminal ossicle at odontoid tip
- Evaluate for atlantoaxial instability if dystopic ossicle, excessive soft tissue pannus, or trisomy 21 patient

*(Left) Sagittal bone CT demonstrates a small ossiculum terminale located adjacent to the odontoid tip. The ossicle is in orthotopic position, and CVJ alignment is normal. (Right) Coronal bone CT confirms orthotopic placement of a small orthotopic ossiculum terminale. Note that there is minimal flattening of the odontoid tip adjacent to the ossicle, supporting classification as a persistent terminal odontoid ossicle.*



*(Left) Sagittal bone CT reveals a small dystopic ossiculum terminale positioned between the odontoid tip and clivus. The odontoid tip has remodeled. (Right) Sagittal bone CT shows subluxation of the anterior C1 ring relative to the nearly normal-sized odontoid process. There is a large dystopic ossiculum terminale. Although debatable, the nearly normal size of the odontoid process favors classification as an ossiculum terminale rather than os odontoideum.*

